2019 Spring

"Phase Equilibria *in* Materials"

04.01.2019

Eun Soo Park

Office: 33-313
Telephone: 880-7221
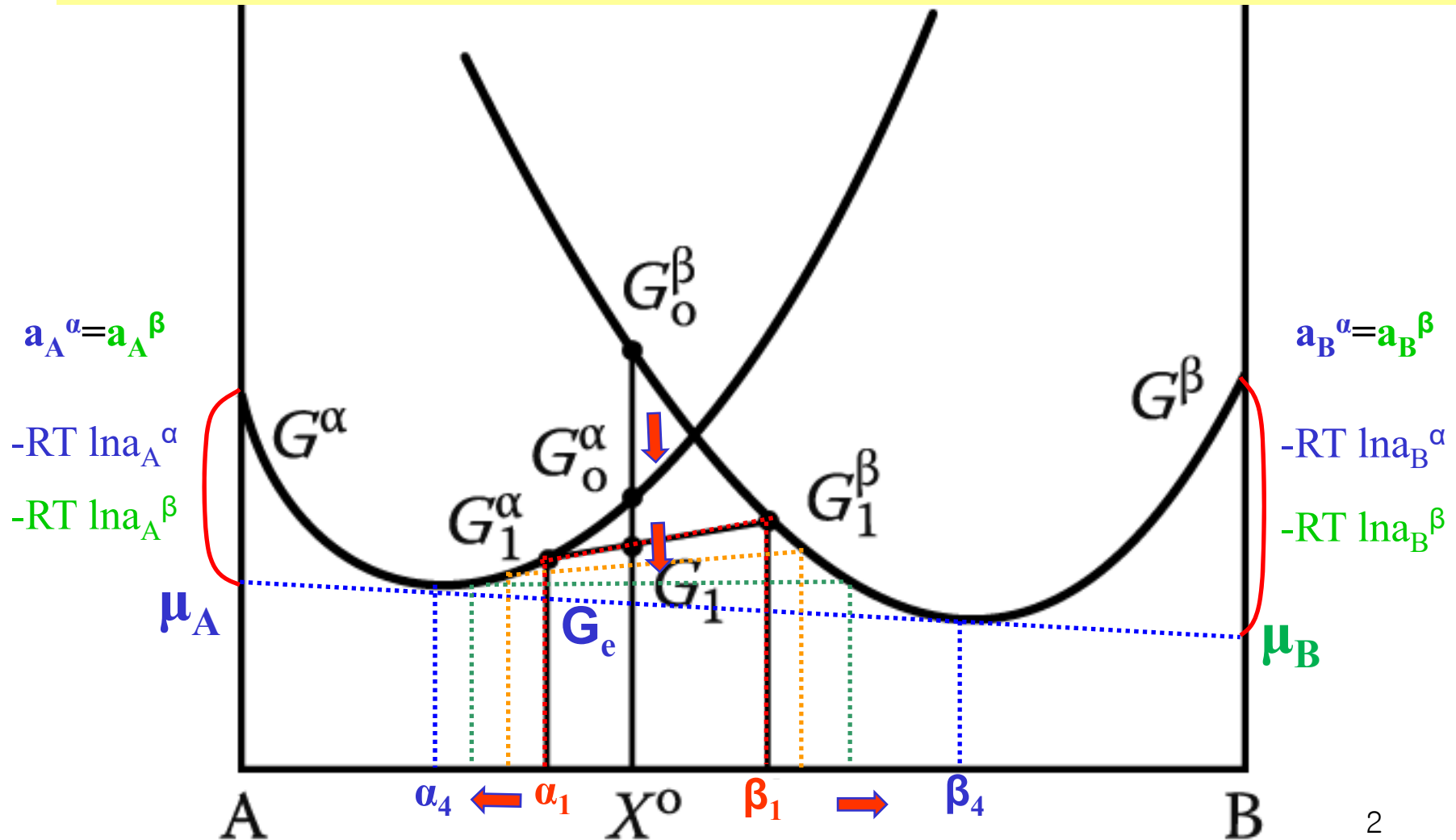**Email: espark@snu.ac.kr**
Office hours: by an appointment

Contents for previous class

Equilibrium in Heterogeneous Systems

In X^0, $G_0^\beta > G_0^\alpha > G_1$ ➡ **α + β separation** ➡ **unified chemical potential**

- Two-Phase Equilibrium

1) Simple Phase Diagrams

Assumption: (1) completely miscible in solid and liquid.
(2) Both are ideal soln. $\Delta H^L_{mix} = 0 \quad \Delta H^S_{mix} = 0$
(3) $T_m(A) > T_m(B)$

Since $S^s \neq S^l$, then $dT/dX_A = 0$. Thus the condition $X^s_A = X^l_A$ is only associated with $dT/dX_A = 0$, *i.e.* with a minimum or a maximum in the line $T_A T_B$ of Fig. 22. Except for this particular case therefore $X^s_A \neq X^l_A$. There is a difference between the composition of the liquid and solid phase in the general case.
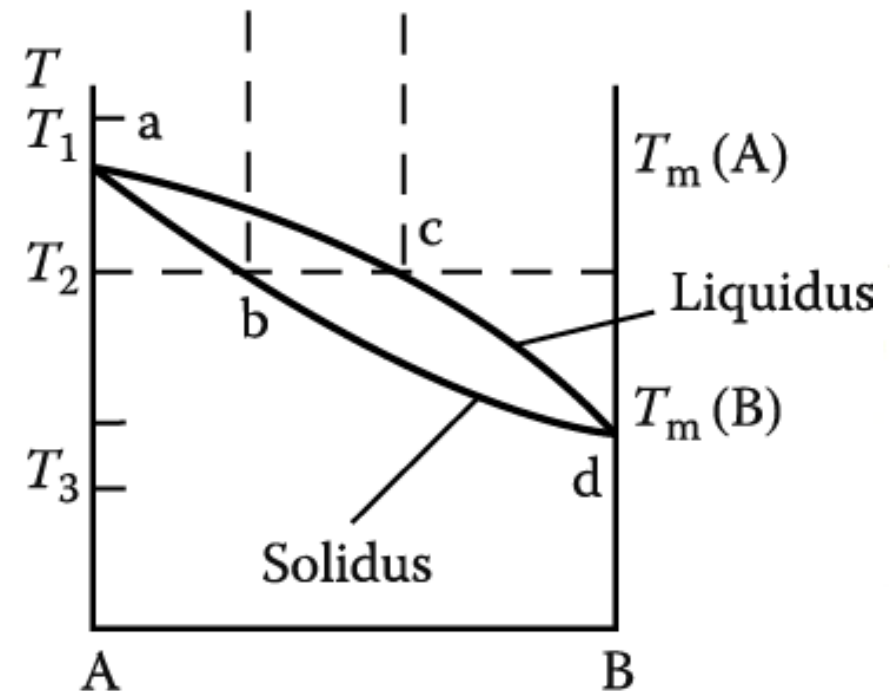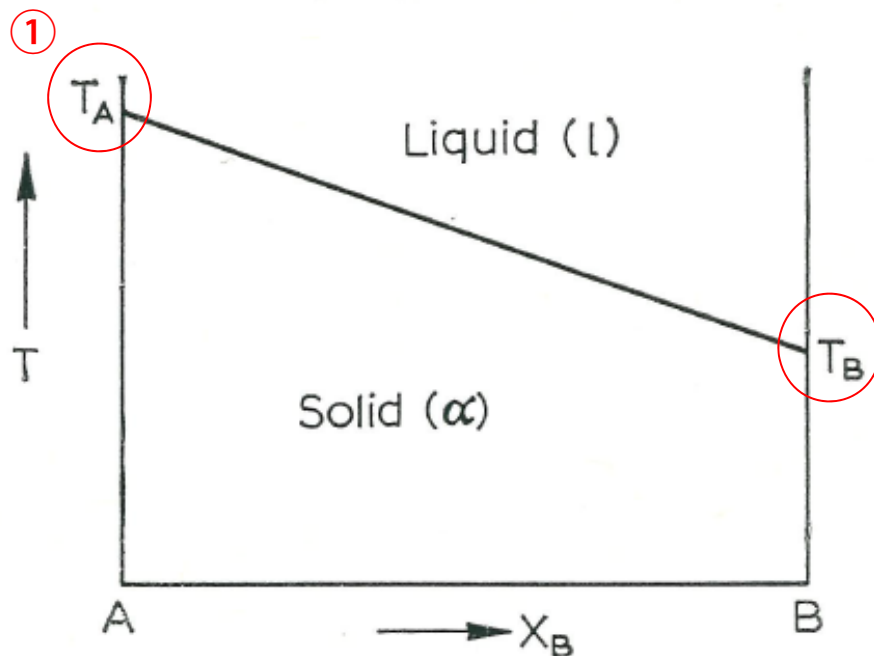
* Consider the free energy curves for liquid and α phase at a temperature T, where $T_A > T > T_B$. The standard states are <u>pure *solid* A</u> and <u>pure *liquid* B</u> at temperature T. → Derive the free energy curves for the liquid and α phases.

② X-T relationship in A-rich and B-rich compositions

As the temperature approaches T_A the quantities X_A^s and X_A^l will approach unity, and $1/T$ will approach $1/T_A$.

Hence near T_A:

$$\ln \frac{X_B^s}{X_B^l} = \frac{\Delta H_B}{R}\left(\frac{1}{T} - \frac{1}{T_B}\right).$$

X-T relationship in A-rich composition

(103)

Similarly, if the temperature approaches T_B, $X_B^s \simeq X_B^l \to 1$ and $1/T \to 1/T_B$. Near T_B:

$$\ln \frac{X_A^s}{X_A^l} = \frac{\Delta H_A}{R}\left(\frac{1}{T} - \frac{1}{T_A}\right).$$

X-T relationship in B-rich composition

(104)

Knowing ΔH_A, ΔH_B, T_A and T_B, the above two equations can be used to determine the compositions of co-existing phases at a series of temperatures, T, between T_A and T_B. **→ Fig. 23*f***

Referring to Fig. 23f, if A is regarded as the solvent, for very dilute solutions of B in A we can write

$$X_A \to 1 \quad \text{and} \quad -\ln X_A \simeq X_B.$$

In terms of eqn. (104):

$$X_A^l - X_A^s = \frac{\Delta H_A}{R} \left(\frac{T_A - T}{T T_A} \right).$$

Since $X_A^l = 1 - X_B^l$ and $X_A^s = 1 - X_B^s$

$$X_B^s - X_B^l = \frac{\Delta H_A}{R} \left(\frac{T_A - T}{T T_A} \right). \qquad (105)$$

As T approaches T_A (in dilute solutions of B in solvent A), the denominator on the right-hand side of eqn. (105) can be written RT_A^2. Therefore

$$X_B^s - X_B^l = \frac{\Delta H_A}{R T_A^2} (T_A - T) \qquad (106)$$

or,

③ ΔH effect for G curvature
 : initial slope of solidus
  and liquidus curve

$$\left(\frac{dX_B^s}{dT} - \frac{dX_B^l}{dT} \right)_{T=T_A} = \frac{\Delta H_A}{R T_A^2}. \qquad (107)$$

Equations (106) and (107) are referred to as the Van't Hoff relation. They give the depression of the freezing point for a liquid solution in equilibrium with a solid solution. The difference in initial slopes of the solidus and liquidus curves, the slopes at $T = T_A$ and $X_A = 1$, are dependent on the latent heat of fusion of pure A (ΔH_A) but independent of the nature of the solute.

* Consider actual (or so-called regular) **solutions**

in which $\Delta H_m \neq 0$, but $\Delta S_m = \Delta S_{m,\text{ideal}}$.

$$\Delta G_m^l = \Delta H_m^l + X_A^l \Delta G_A + RT(X_A^l \ln X_A^l + X_B^l \ln X_B^l).$$

Since

$$\Delta G_A = \Delta H_A - T\Delta S_A$$

then,

$$\Delta G_m^l = \Delta H_m^l + X_A^l \Delta H_A - \boxed{X_A^l T\Delta S_A} + RT(X_A^l \ln X_A^l + X_B^l \ln X_B^l).$$

The free energy curve for the solid phase is:

$$\Delta G_m^s = \Delta H_m^s - X_B^s \Delta G_B + RT(X_A^s \ln X_A^s + X_B^s \ln X_B^s)$$

or,

$$\Delta G_m^s = \Delta H_m^s - X_B^s \Delta H_B + \boxed{X_B^s T\Delta S_B} + RT(X_A^s \ln X_A^s + X_B^s \ln X_B^s).$$

④ Temperature effect for G variation
: role of ΔS

6

1) Simple Phase Diagrams **a) Variation of temp.: $G^L > G^s$**

b) T ↓ → Decrease of curvature of G curve

(∵ decrease of -TΔS$_{mix}$ effect)

Fig. 26. Free energy curves for liquid and solid phases in the U–Zr system at 1500°, 1800° and 2000 °K. It was assumed that $\Delta H_m^l = \Delta H_m^s$

1.5 Binary phase diagrams
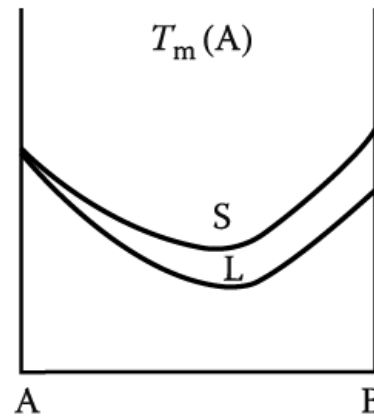
1) Simple Phase Diagrams

Assumption:
(1) completely miscible in solid and liquid.
(2) Both are ideal soln.
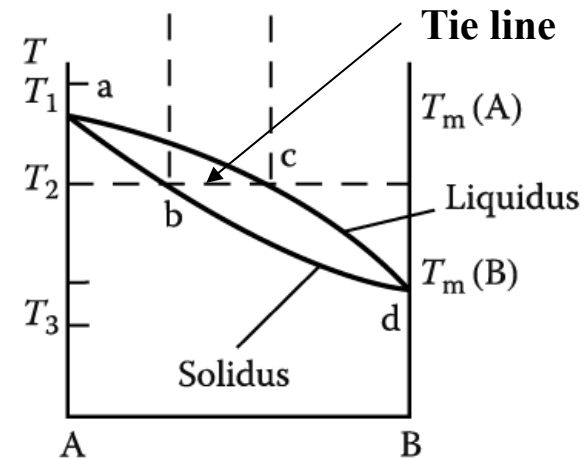(3) $T_m(A) > T_m(B)$
(4) $T_1 > T_m(A) > T_2 > T_m(B) > T_3$

a) Variation of temp.: $G^L > G^S$
b) $T \downarrow \rightarrow$ Decrease of curvature of G curve
(∵ decrease of $-T\Delta S_{mix}$ effect)

(a) T_1 (b) $T_m(A)$ (c) T_2

(d) $T_m(B)$ (e) T_3 (f)

Tie line
Liquidus
Solidus
$T_m(A)$
$T_m(B)$
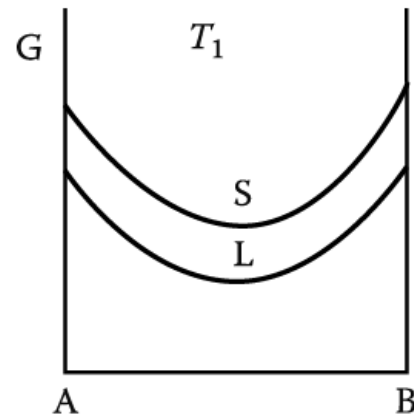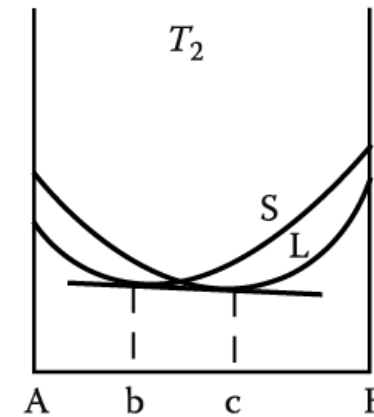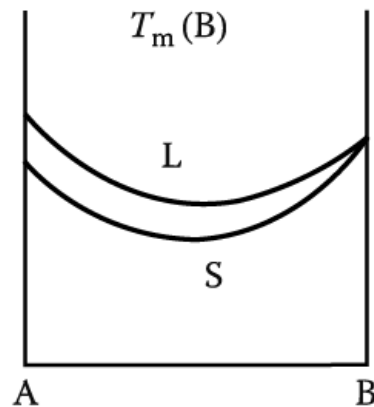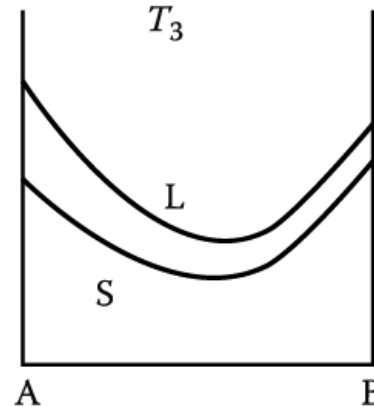
Contents for today's class

- Equilibrium in Heterogeneous Systems

$G_0^\beta > G_0^\alpha > G_0^{\alpha+\beta}$ ⟹ **α + β separation** ⟹ **unified chemical potential**

- Binary phase diagrams

1) Simple Phase Diagrams

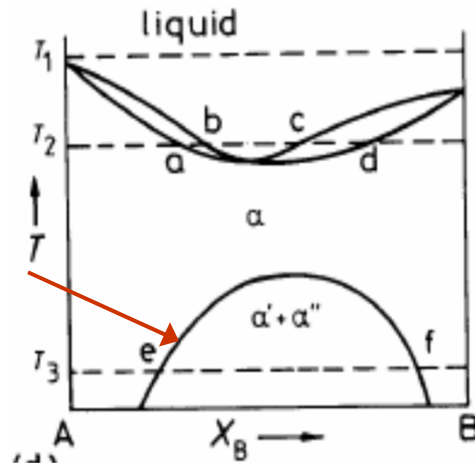$$\Delta H_{mix}^L = 0 \quad \Delta H_{mix}^S = 0$$

Assume: (1) completely miscible in solid and liquid.
(2) Both are ideal soln.
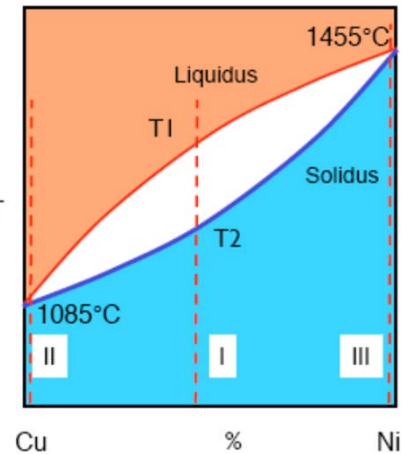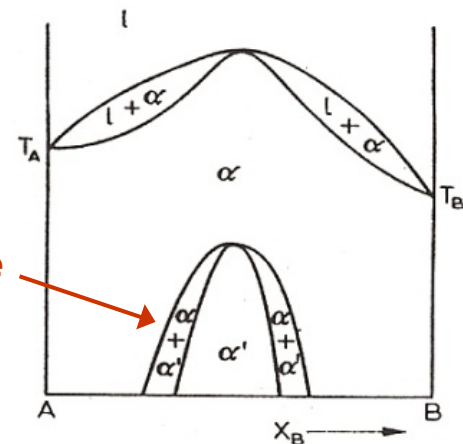

2) Variant of the simple phase diagram

$$\Delta H_{mix}^\alpha > \Delta H_{mix}^l > 0$$

$$\Delta H_{mix}^\alpha < \Delta H_{mix}^l < 0$$

miscibility gab

Ordered phase

9

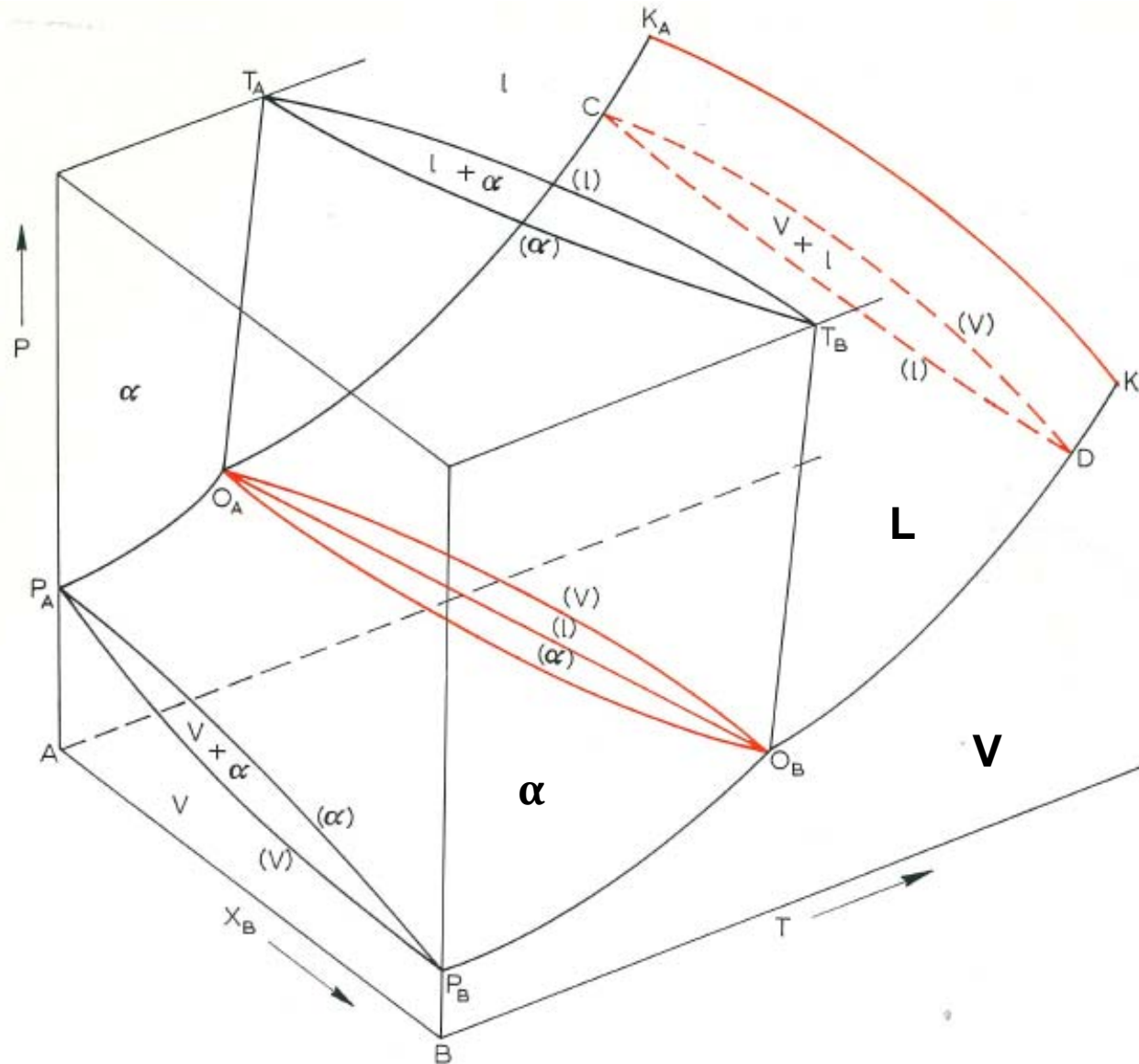# 3.2.6 Pressure-Temperature-Composition phase diagram for a system with continuous series of solutions

Fig. 35. Pressure–temperature–composition phase diagram for a system with continuous series of solutions

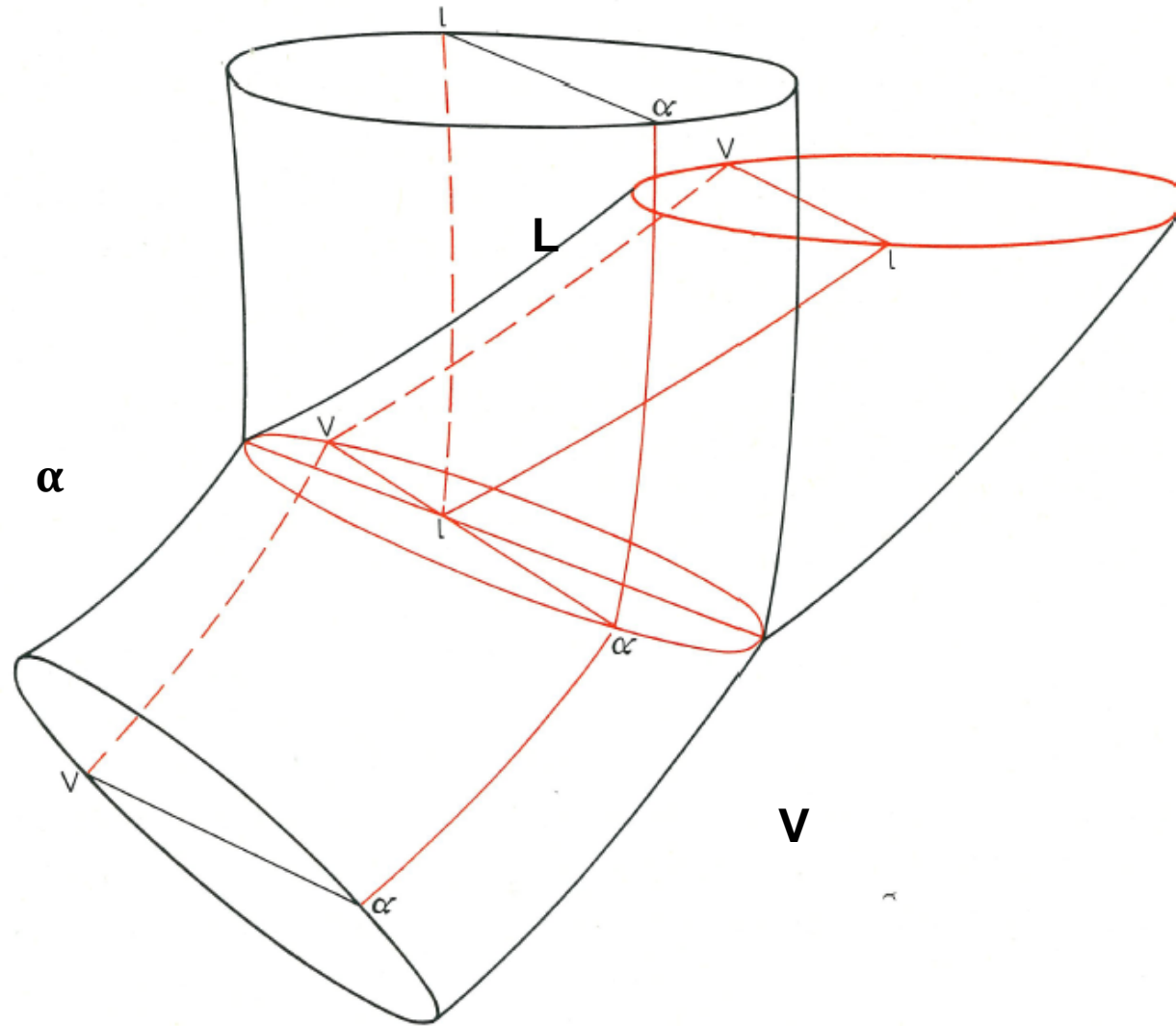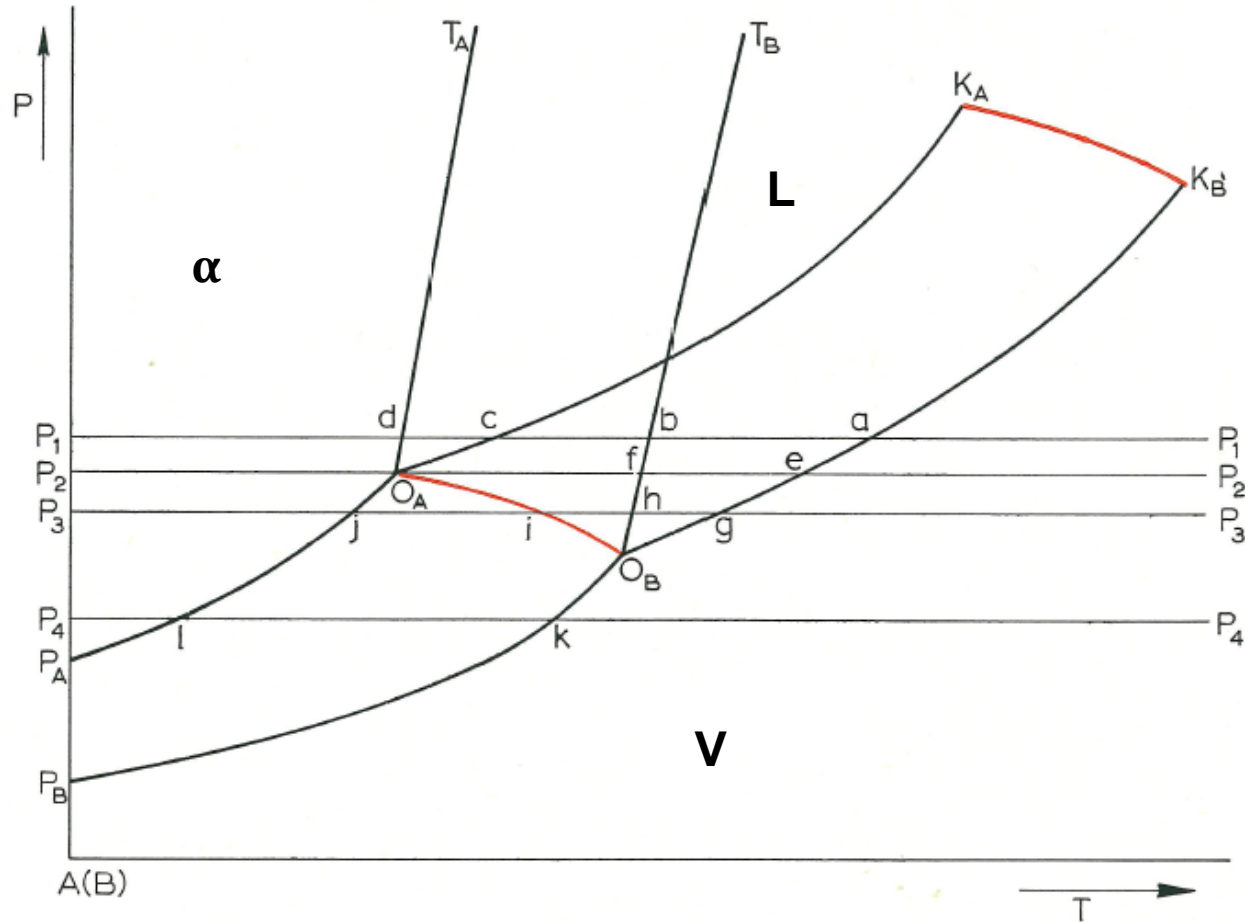# 3.2.6 Pressure-Temperature-Composition phase diagram for a system with continuous series of solutions

Fig. 36. Formation of a three-phase tie line $Vl\alpha$.

3.2.6 Pressure-Temperature-Composition phase diagram for a system with continuous series of solutions

Fig. 37. Two-dimensional projection of Fig. 35 on the P–T plane for component A.

$P_A O_A$ — equilibrium between V_A and α_A; $P_B O_B$ — V_B and α_B; $O_A T_A$ — l_A and α_A; $O_B T_B$ — l_B and α_B; $O_A K_A$ — V_A and l_A; $O_B K_B$ — V_B and l_B; $O_A O_B$ — V_{AB}, l_{AB} and α_{AB}; O_A — V_A, l_A and α_A; O_B — V_B, l_B and α_B; $K_A K_B$ — $V_{AB} = l_{AB}$.

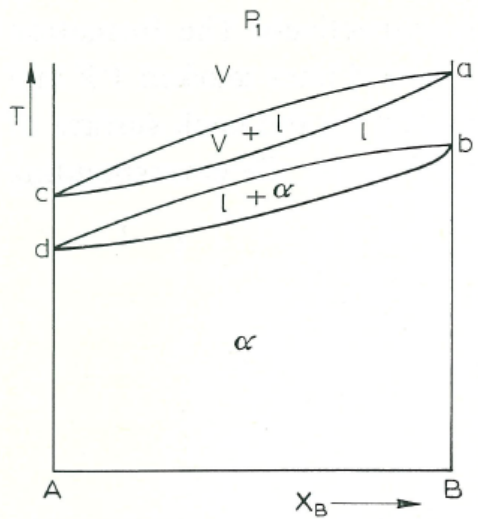# 3.2.6 Pressure-Temperature-Composition phase diagram for a system with continuous series of solutions

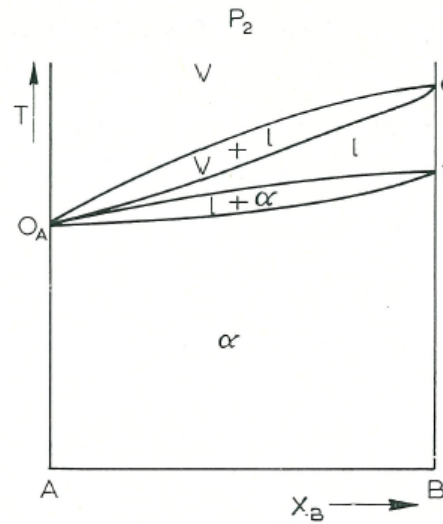Fig. 38. T–X section through Fig. 35 at a pressure P_1 where $K_B > P_1 > O_A$.

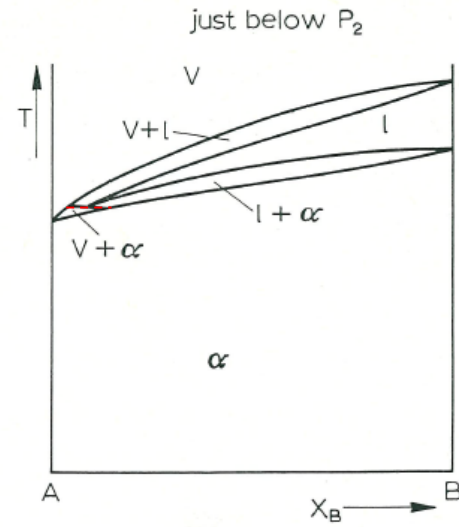Fig. 39. T–X section through Fig. 35 at a pressure P_2 where $P_2 = O_A$

Fig. 40. T–X section through Fig. 35 at a pressure just below P_2.
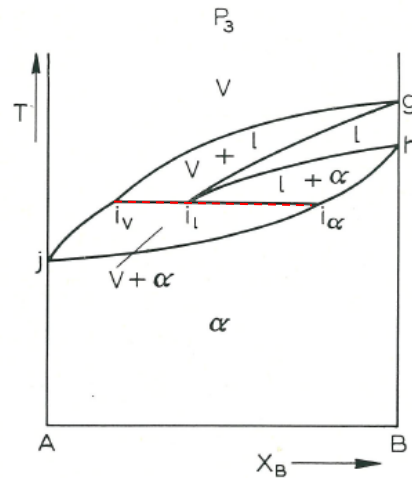
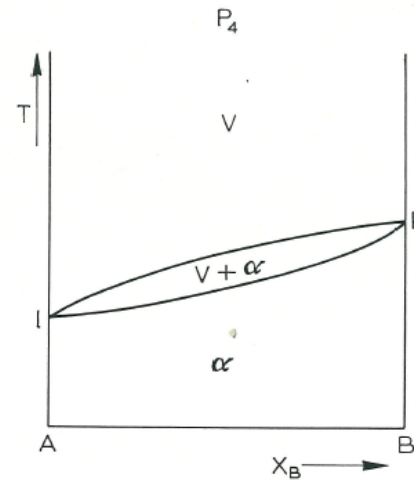Fig. 41. T–X section through Fig. 35 at a pressure P_3 where $O_A > P_3 > O_B$.

Fig. 42. T–X section through Fig. 35 at a pressure P_4 where $O_B > P_4 > P_B$.

13

Contents for today's class

CHAPTER 4
Binary Phase Diagrams

Three-Phase Equilibrium Involving Limited Solubility of the Components in the Solid State but Complete Solubility in the Liquid State

* Three-Phase Equilibrium : Eutectic Reactions

a) Structural Factor: Hume-Rothery Rules

Empirical rules for substitutional solid-solution

complete solid solution ⟷ limited solid solution

Similar atomic radii, the same valency and crystal structure

b) The eutectic reaction

c) Limiting forms of eutectic phase diagrams

d) Retrogade solidus curves

* Simple Eutectic Systems $\Delta H^{\alpha}_{mix} > \Delta H^{l}_{mix} > 0$

- **Three-Phase Equilibrium Involving Limited Solubility of the Components in the Solid State but Complete Solubility in the Liquid State**
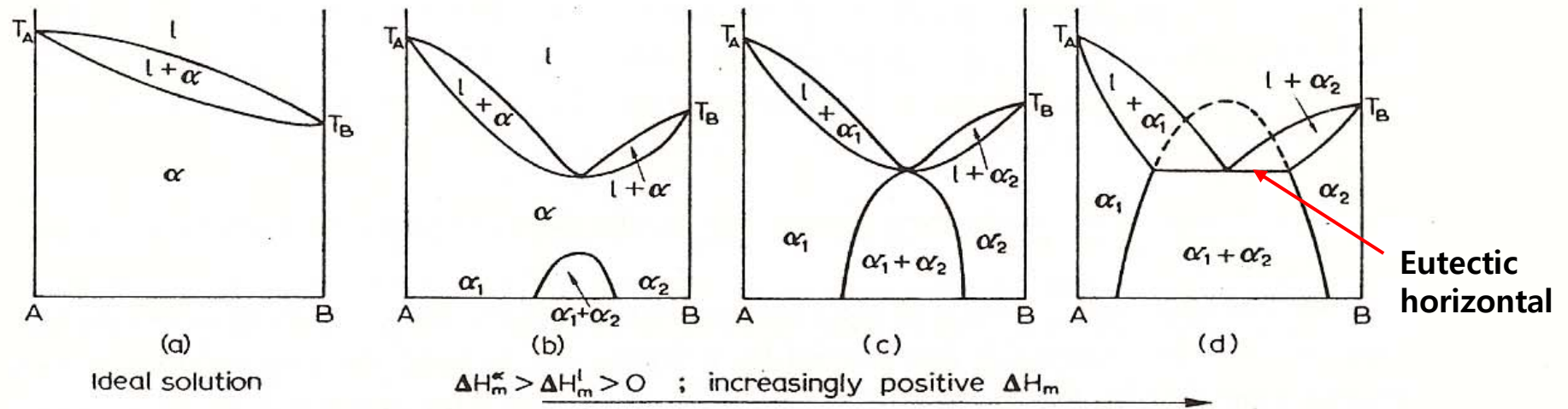

Fig. 43. Effect of increasingly positive departure from ideality in changing the phase diagram for a continuous series of solutions to a eutectic-type.

* Simple Eutectic Systems

- **$\Delta H_m >> 0$ and the miscibility gap extends to the melting temperature. (when both solids have the same structure.)**
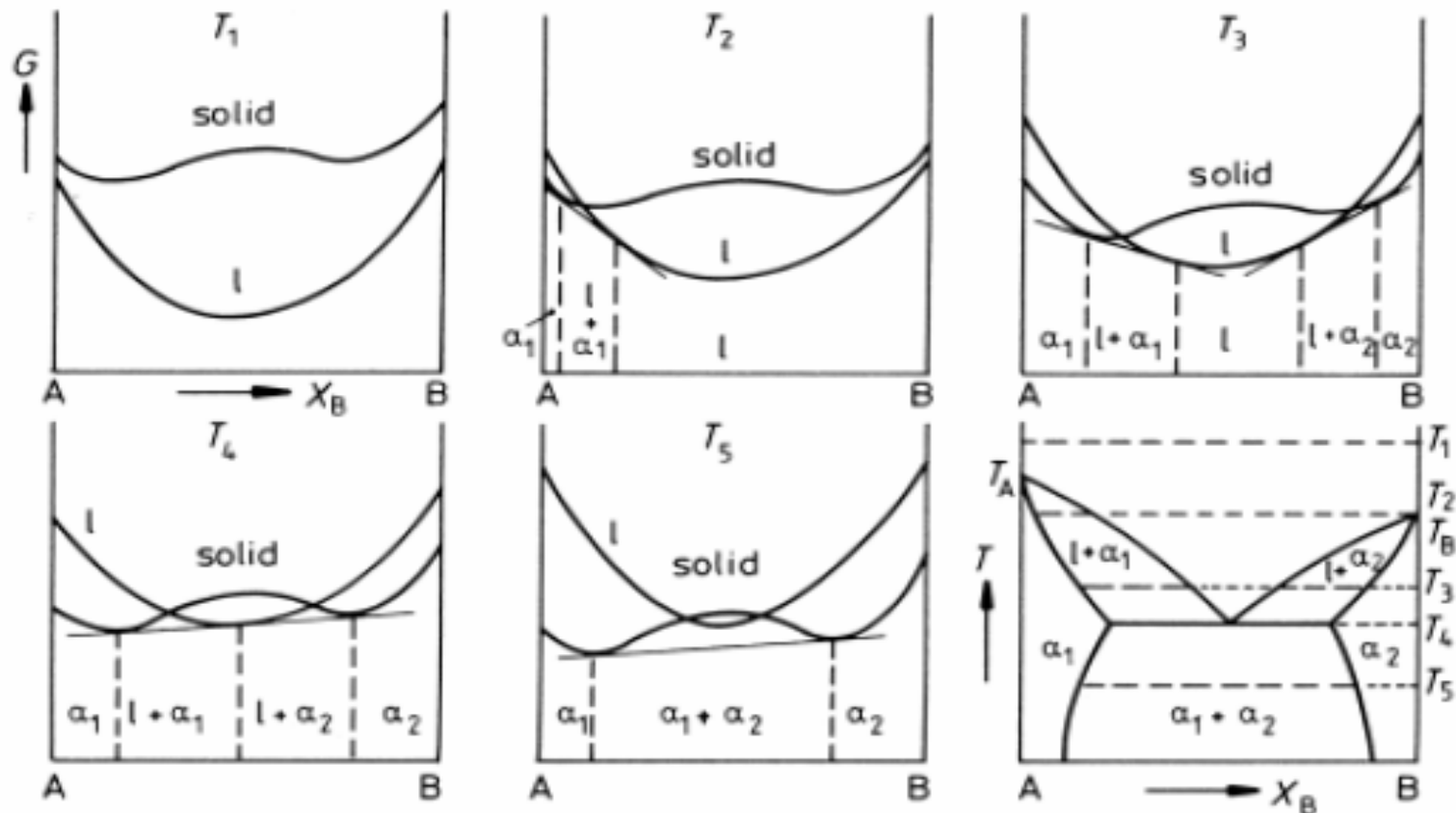

Fig 1.32 The derivation of a eutectic phase diagram where both solid phases have the same crystal structure. (After A.H. Cottrell, *Theoretical Structural Metallurgy*, Edward Arnold, London, 1955,©Sir Alan Cottrell.)
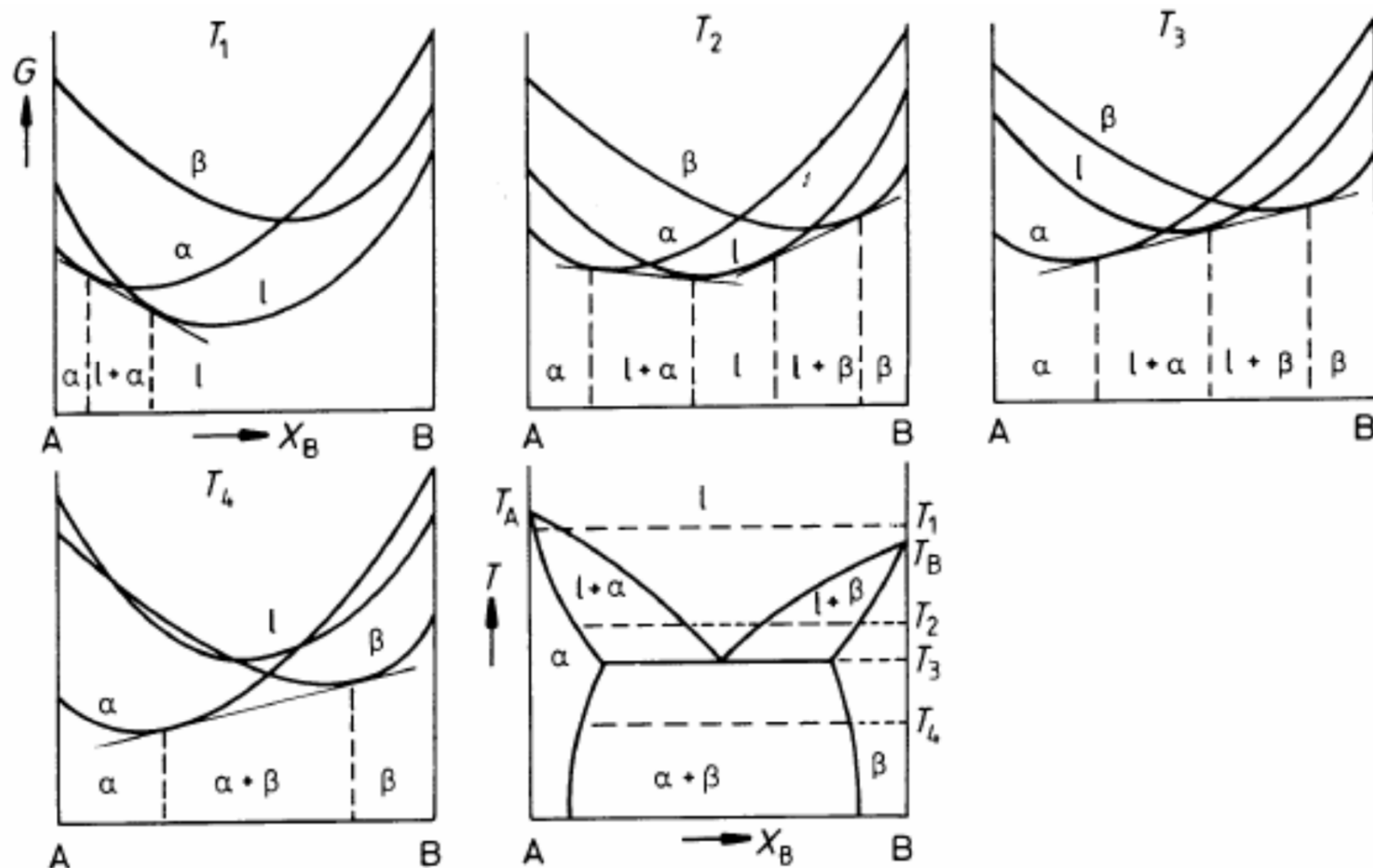
(when each solid has the different crystal structure.)
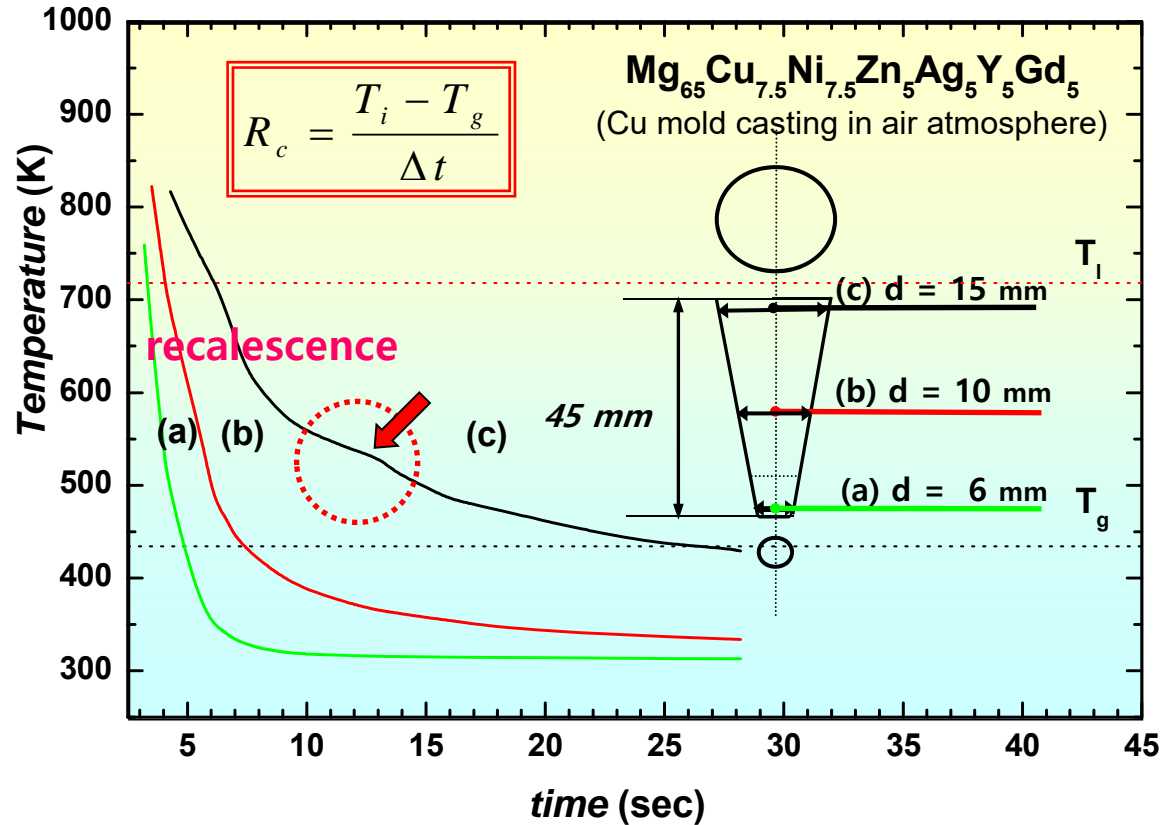

Fig. 1.33 The derivation of a eutectic phase diagram where each solid phase has a different crystal structure. (After A. Prince, *Alloy Phase Equilibria*, Elsevier, Amsterdam, 1966.)

# Measurement of R_c in Mg BMG (D_{max}=14 mm)

$$R_c = \frac{T_i - T_g}{\Delta t}$$

$Mg_{65}Cu_{7.5}Ni_{7.5}Zn_5Ag_5Y_5Gd_5$
(Cu mold casting in air atmosphere)

T_l

recalescence

(a) (b)   (c)   45 mm

(c) d = 15 mm
(b) d = 10 mm
(a) d = 6 mm T_g

top position : recalescence

middle position : 64K/s

bottom position : 137 K/s

Temperature (K)

time (sec)

* **Cooling curves** measured at the center of the three transverse cross sections

* JAP 104, 023520 (2008)

Nucleation Theory as Applied to solidification
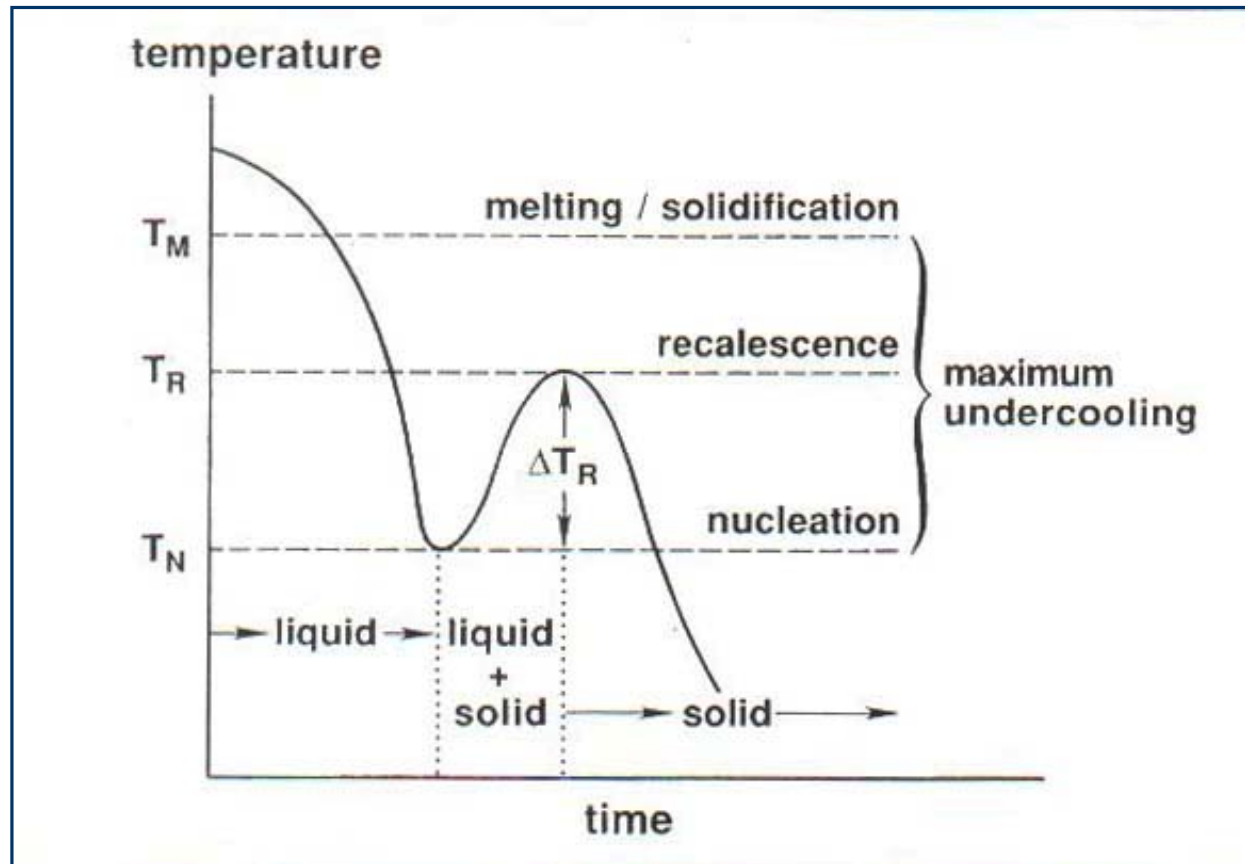
- The recalescence process is illustrated by a temperature versus time plot, showing **the temperature rise on nucleation due to release of the heat of fusion.**
- **A sudden glowing in a undercooled liquid of metal** caused by liberation of the latent heat of transformation
- The higher the recalescence temperature, the larger the microstructural scale in the solid.
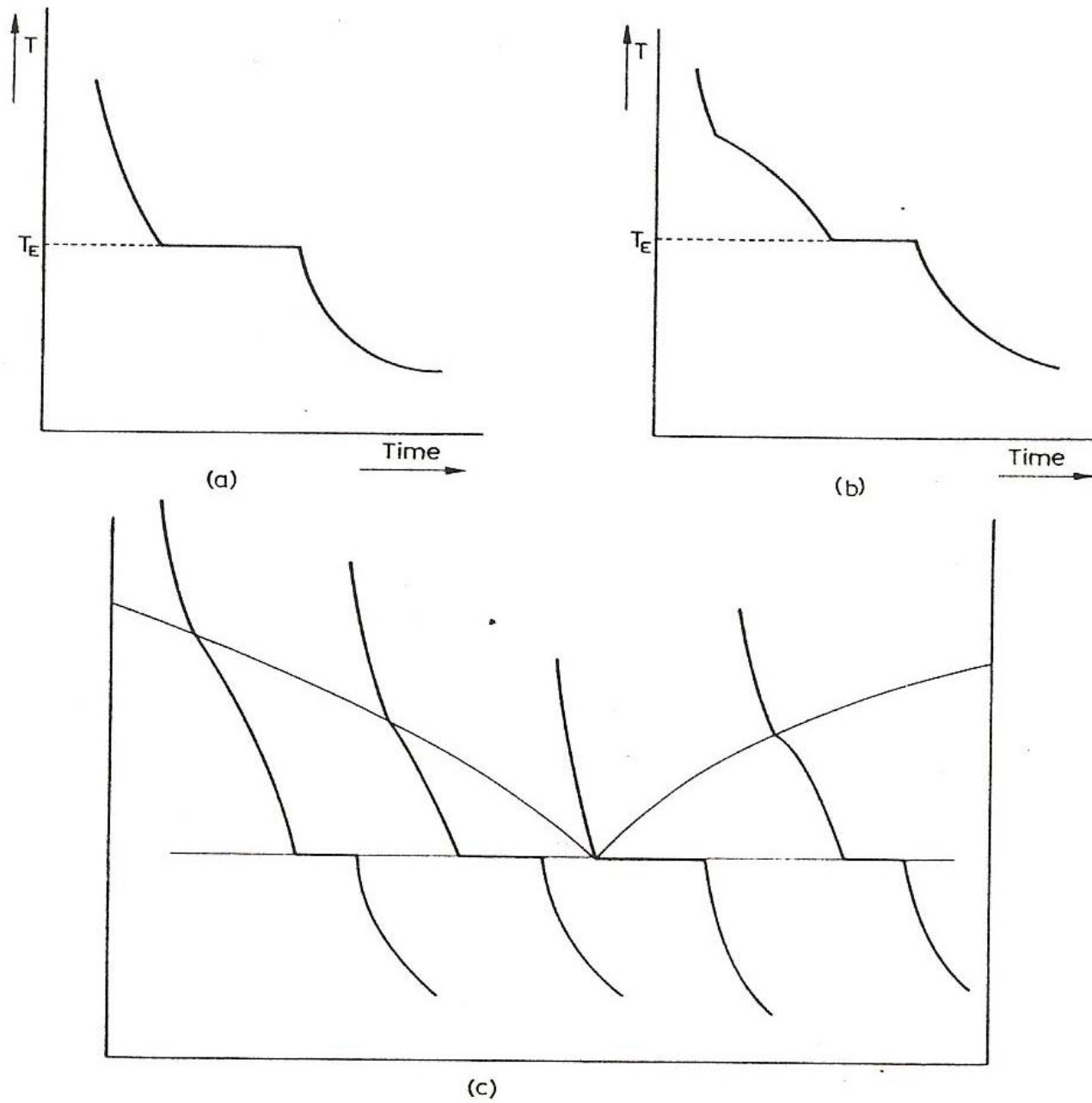
Fig. 48. Cooling curve for (a) the eutectic alloy, (b) hypo-eutectic alloy N, and (c) a series of alloys, allowing the determination of the liquidus and eutectic horizontal.

20

1.5 Binary phase diagrams

Eutectic Systems

$$\Delta H^{L}_{mix} = 0 \quad \Delta H^{S}_{mix} >> 0$$

The Pb-Sn system is characteristic of a valley in the middle. Such system is known as the **Eutectic** system. The central point is the Eutectic point and the transformation though this point is called Eutectic reaction: **L ✦ α+β**

Pb has a fcc structure and Sn has a tetragonal structure. The system has three phases: L, α and β.

Pb-Sn phase diagram

- Liquid
- Liquidus
- α + L
- Eutectic point
- L + β
- solidus
- α phase: solid solution of Sn in fcc Pb
- β phase: solid solution of Pb in tetragonal Sn
- solvus
- α + β
- solvus

Temperature axis: 0, 50, 100, 150, 200, 250, 300, 350

Wt% axis: 0 (Pb, Fcc), 10, 20, 30, 40, 50, 60, 70, 80, 90, 100 (Sn, Tetra)
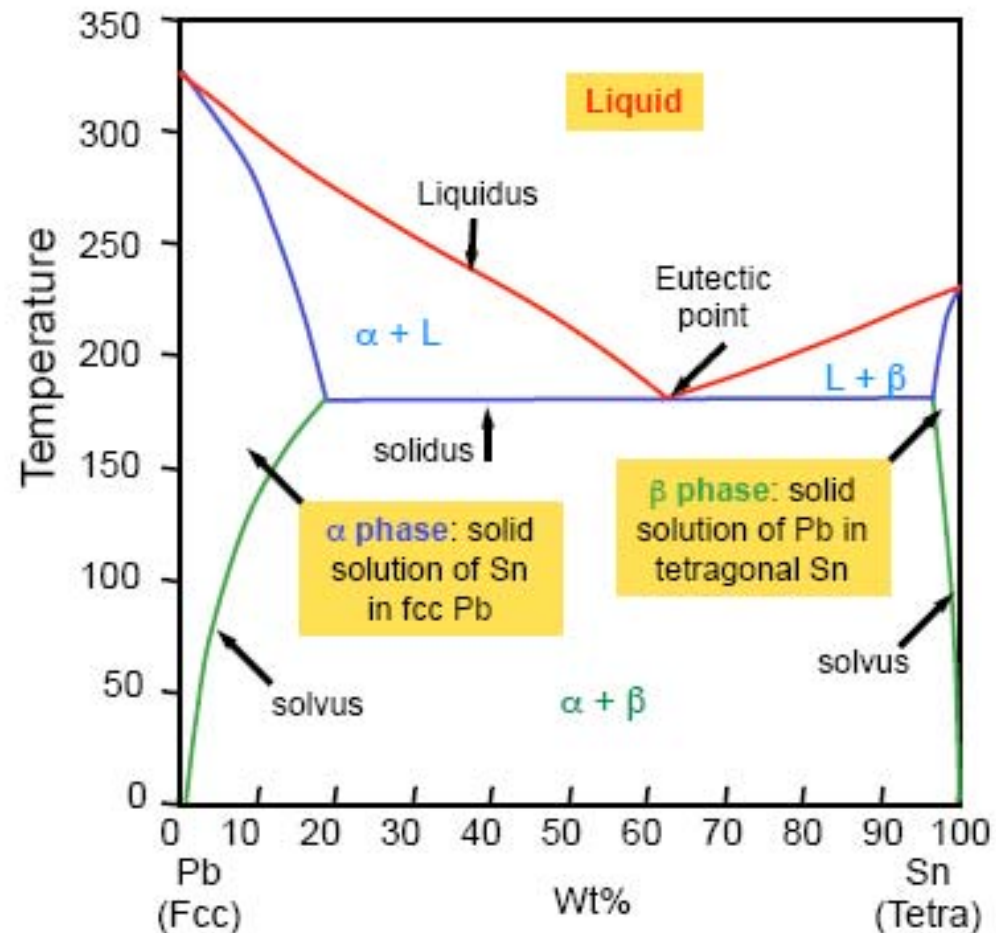
1.5 Binary phase diagrams

Solidification of Eutectic Systems

Alloy II

At point 1: Liquid

Solidification starts at eutectic point (where liquidus and solidus join)

At point 2: $L \blacklozenge (\alpha + \beta)$ (eutectic reaction)

The amounts of α and β increase in proportion with time.

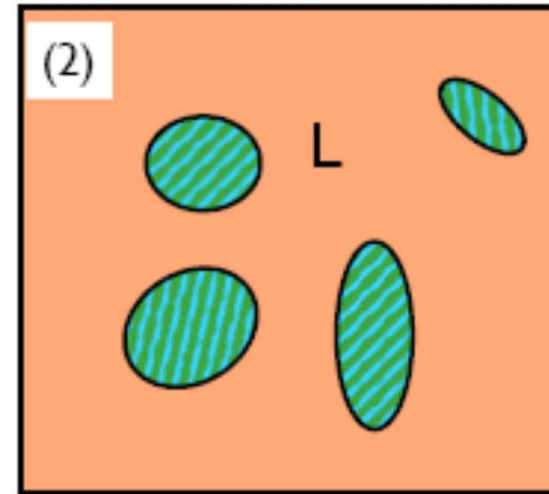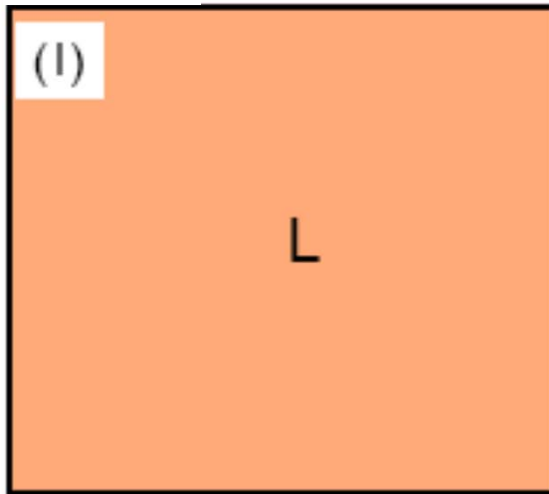Solidification finishes at the same temperature.

At point 3: $\alpha + \beta$

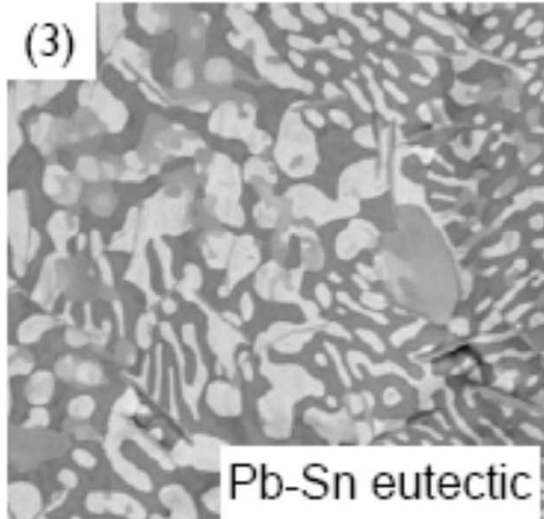Further cooling leads to the depletion of Sn in α and the depletion of Pb in β.
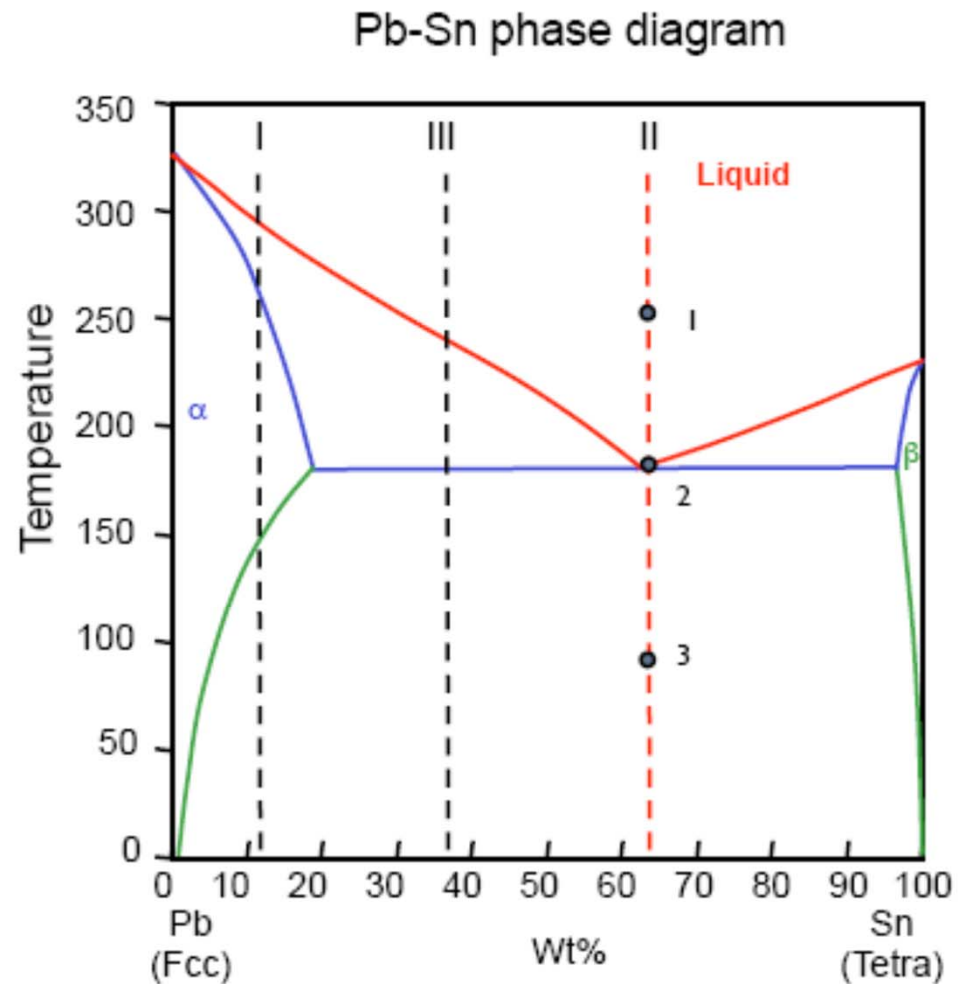
Pb-Sn phase diagram

1.5 Binary phase diagrams

Alloy II

(1) L

(2) L — Nucleation of colonies of α and β laminates

(3) Pb-Sn eutectic — Eutectic structure of intimate mix of α and β to minimise diffusion path

4.3.2 Eutectic Solidification: L→α + β
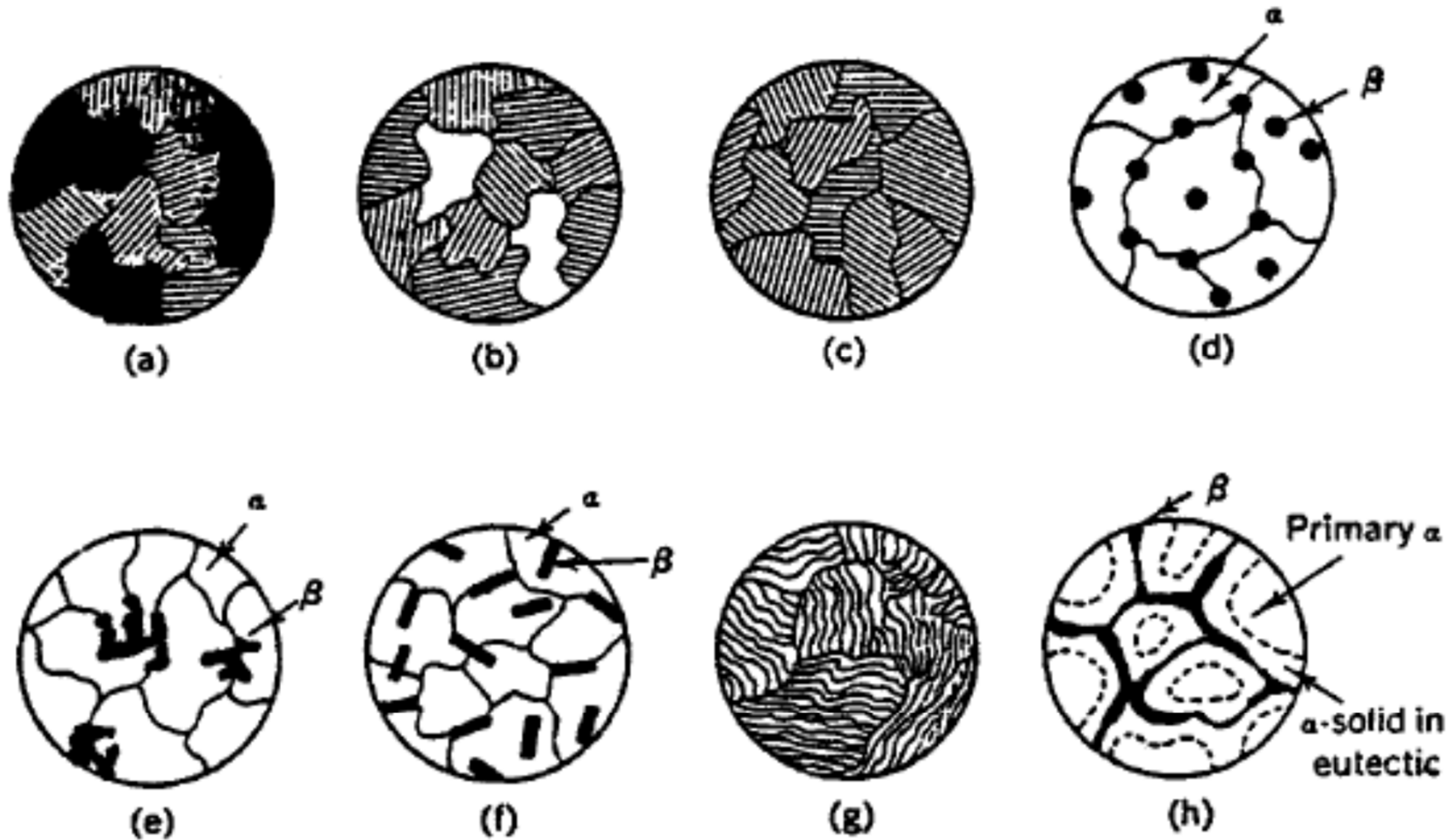
Fig. 14 Schematic representation possible in eutectic structures. (a), (b) and (c) are alloys shown in fig. 13; (d) nodular; (e) Chinese script; (f) acicular; (g) lamellar; and (h) divorced.

4.3.2 Eutectic Solidification

During solidification both phases grow simultaneously behind an essentially planar solid/liquid interface.

Normal eutectic	Anomalous eutectic

Normal eutectic

both phases have low entropies of fusion.

Anomalous eutectic

One of the solid phases is capable of faceting, i.e., has a high entropy or melting.

Fig. 4.30 Rod-like eutectic. Al_6Fe rods in Al matrix. Transverse section. Transmission electron micrograph (x 70000).
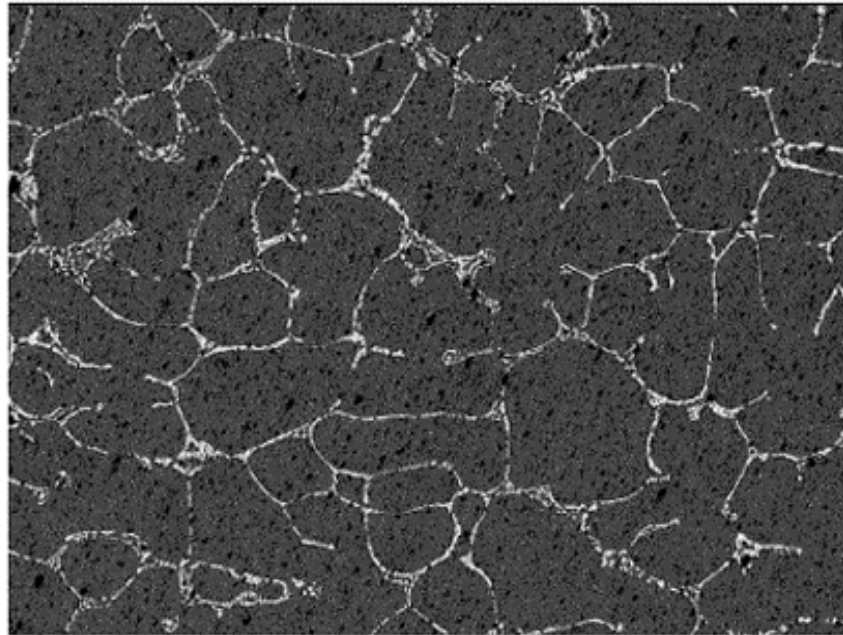
The microstructure of the Pb-61.9%Sn (eutectic) alloy presented a coupled growth of the (Pb)/βSn eutectic. There is a remarkable change in morphology increasing the degree of undercooling with transition from regular lamellar to anomalous eutectic. **25**

http://www.matter.org.uk/solidification/eutectic/anomalous_eutectics.htm

Eutectic

Divorced Eutectic
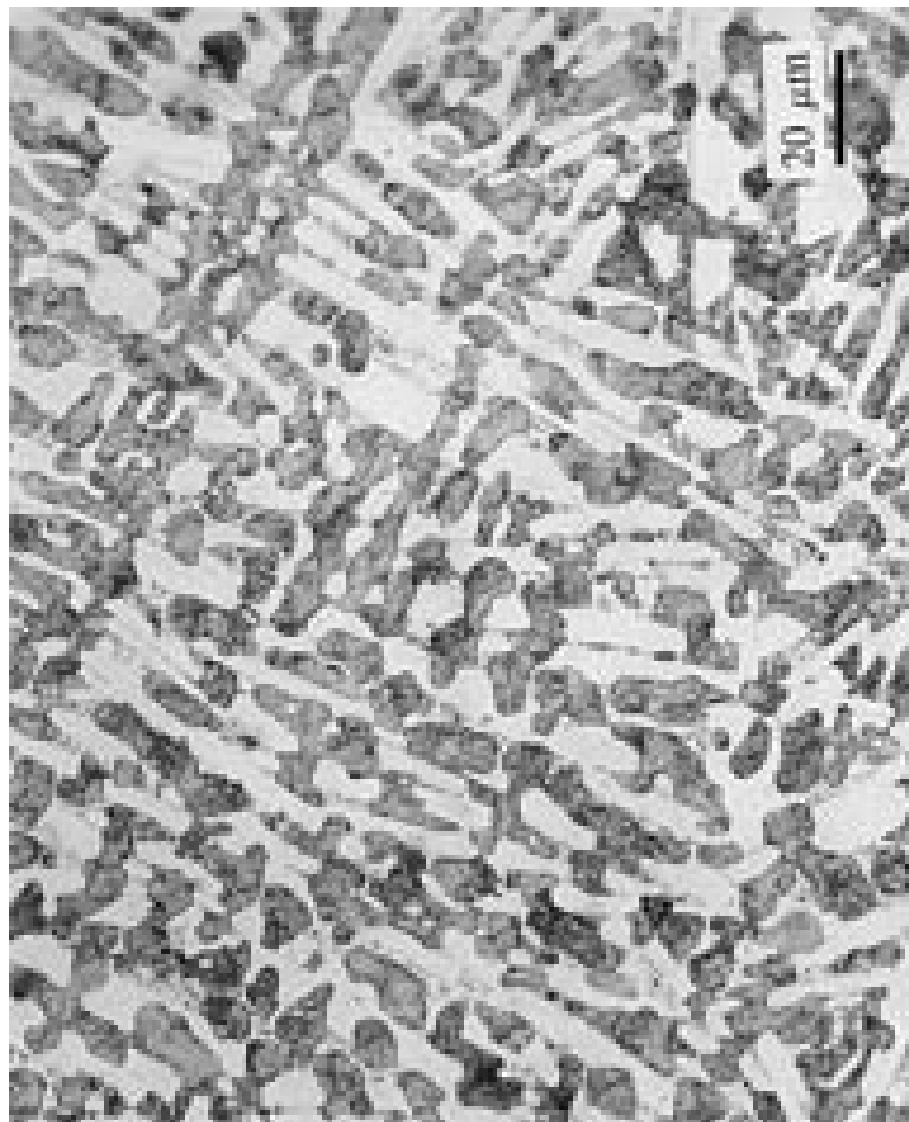
Solidification of Eutectic Systems

Alloy I :

At point 1: Liquid
Solidification starts at liquidus
At point 2: L+α
The amount α ↑ with ↓ T
Solidification finishes at solidus
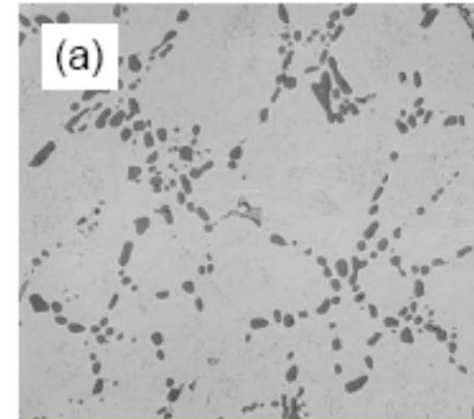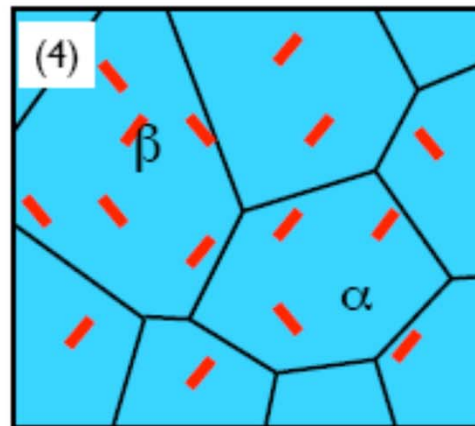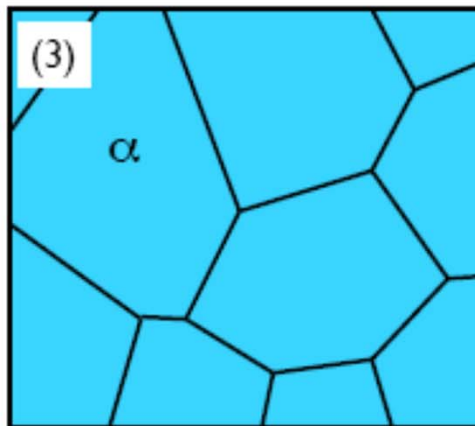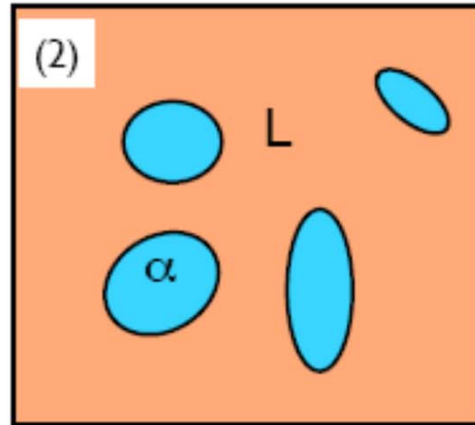At point 3: α
Precipitation starts at solvus
At point 4: α+β
Further cooling leads to formation
and growth of more β precipitates
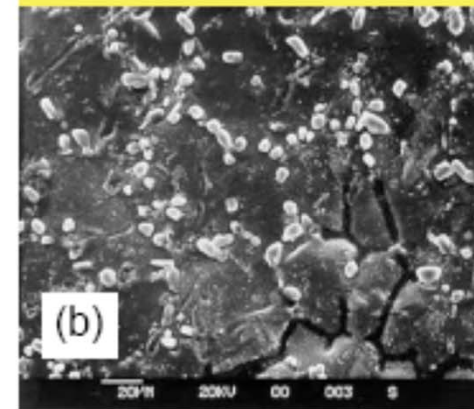whereas Sn% in α decreases
following the solvus.

Pb-Sn phase diagram
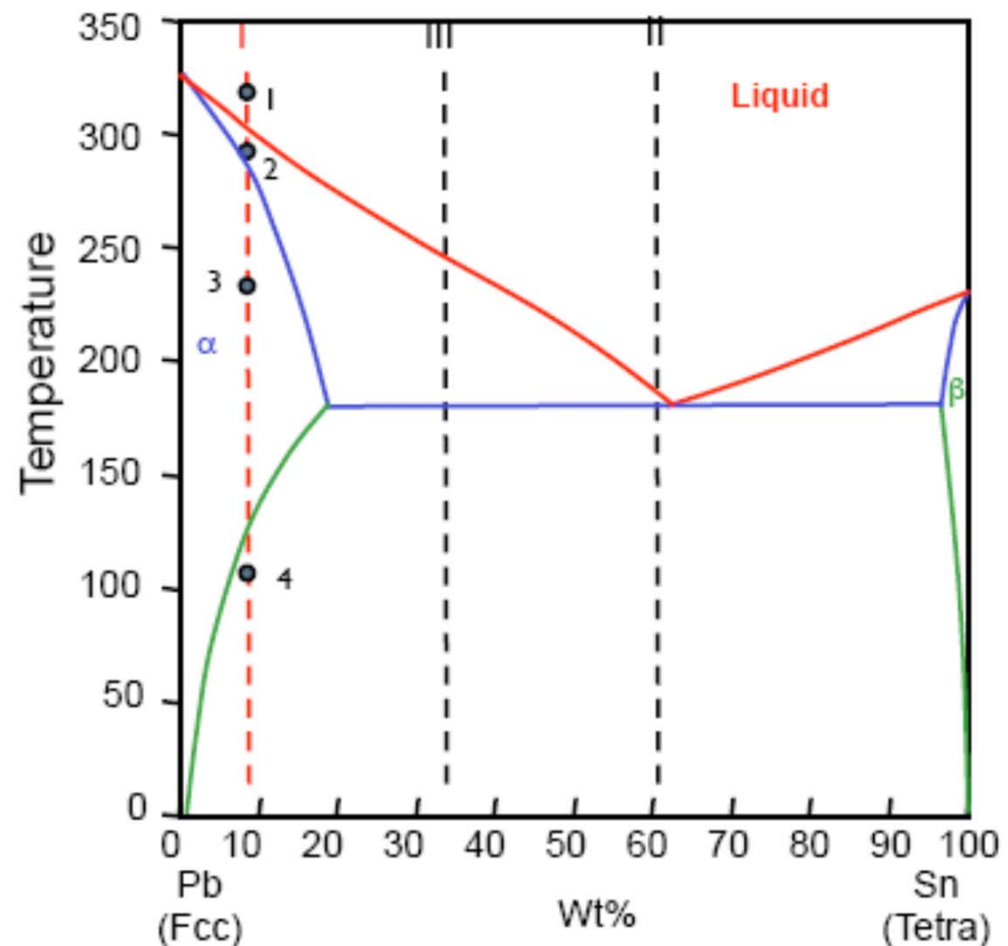
1.5 Binary phase diagrams

Alloy I

Precipitates in a Al-Si alloy;
(a) optical microscopy,
(b) scanning electron
microscopy of fracture surface

1.5 Binary phase diagrams

Solidification of Eutectic Systems

Alloy III

At point 1: Liquid
Solidification starts at liquidus
At point 2: L → L+α (pre-eutectic α)
The amount α ↑ with ↓T
At point 3: L → (α+β) (eutectic reaction)
Solidification finishes at the eutectic temperature
At point 4: α+β (pre-eutectic α + (α+β) eutectic mixture)
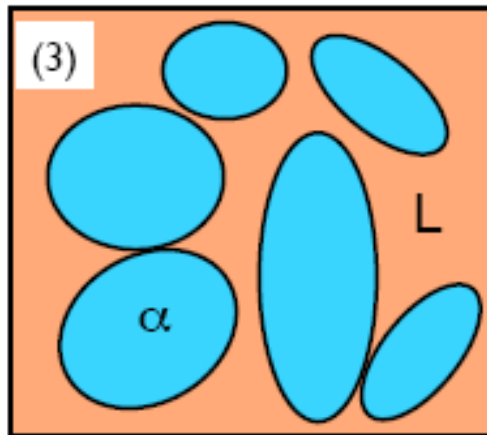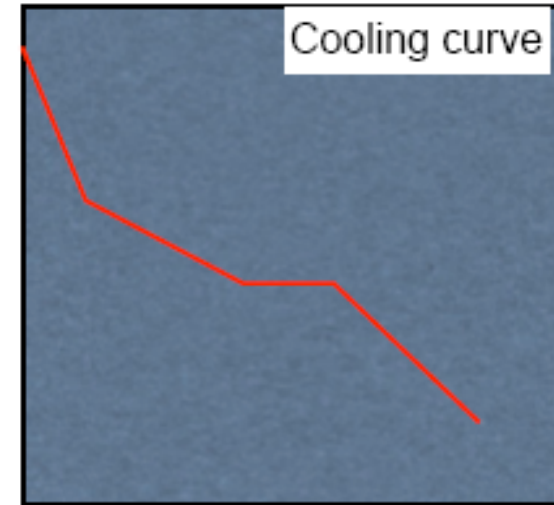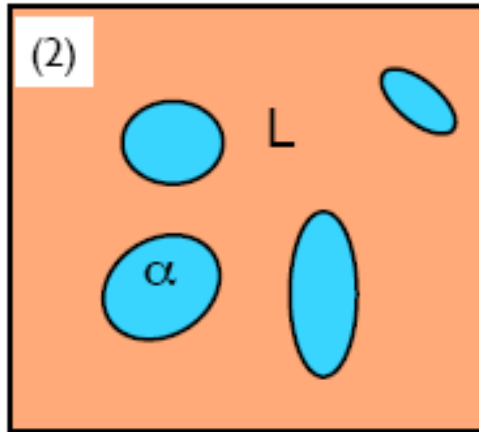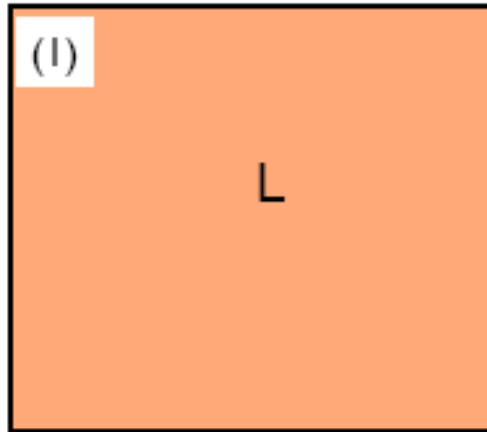Further cooling leads to the depletion of Sn in α and the depletion of Pb in β.

The cooling curve of this alloy is a combination of the two cooling curves shown in slide 9.

Pb-Sn phase diagram
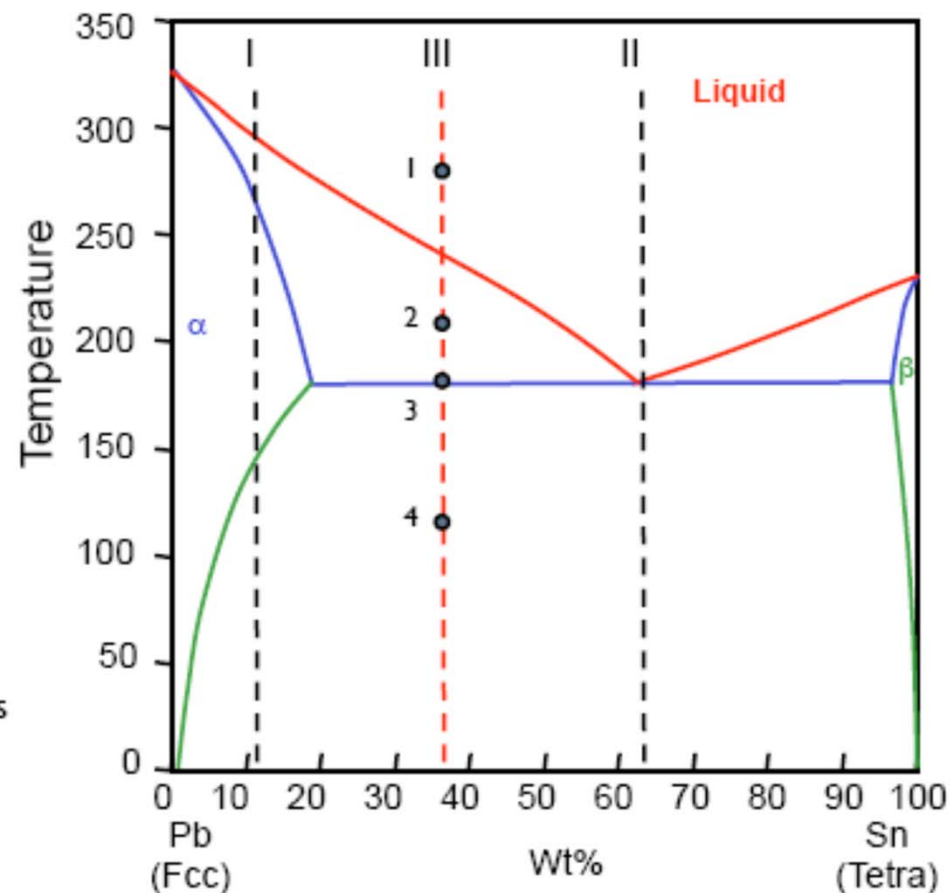
1.5 Binary phase diagrams: Hypoeutectic
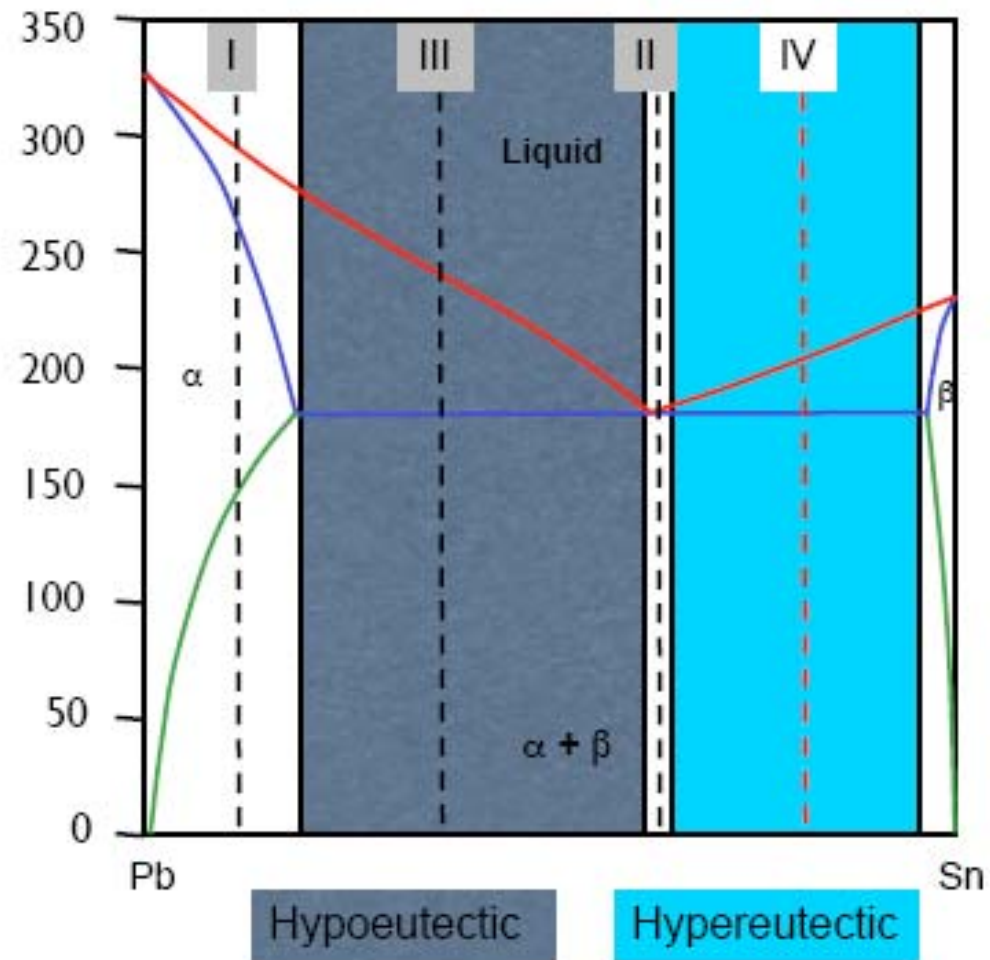
Alloy III

(I) L

(2) L α

Cooling curve

(3) L α

(4) Eut α

Cu-Ag alloy
Pre-eutectic α
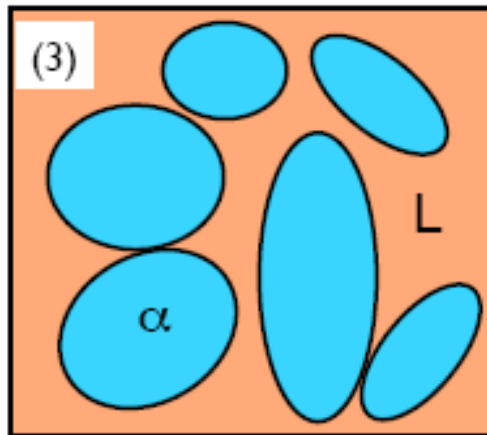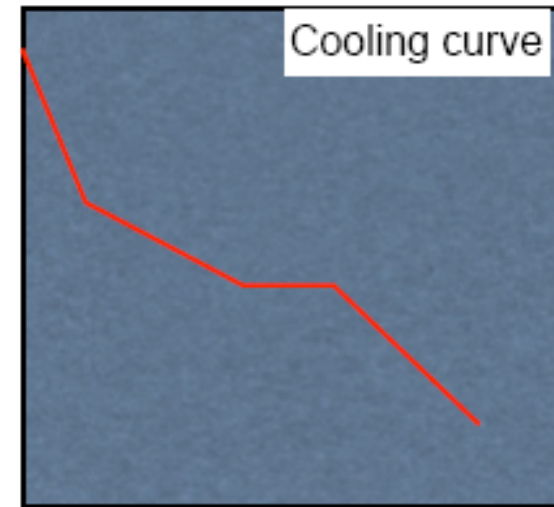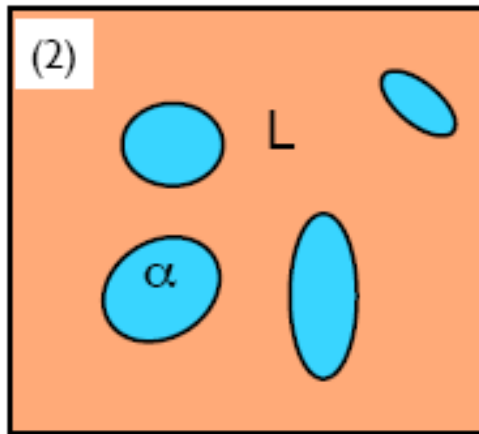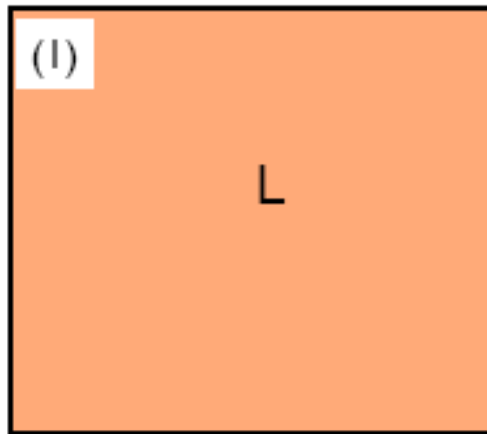Eutectic laminate of α and β
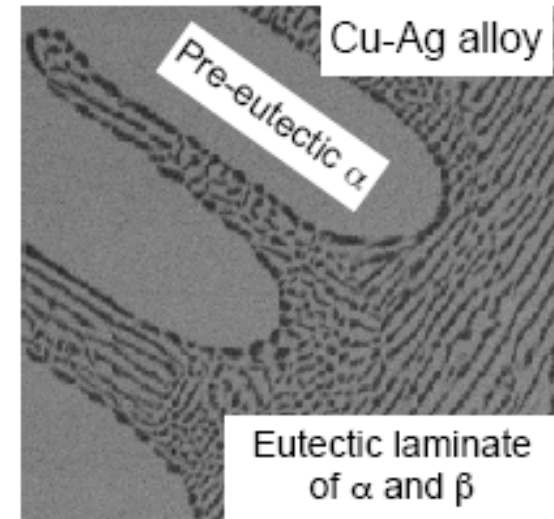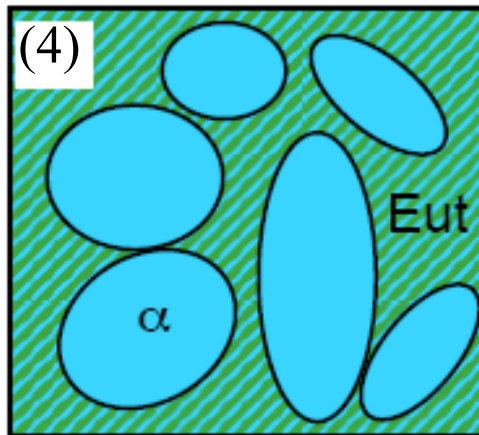
Solidification of Eutectic Systems

Alloy IV

Can you describe the solidification process of alloy IV, including microstructure evolution, morphology of phases and cooling curve?

1.5 Binary phase diagrams : Hypereutectic

Alloy IV
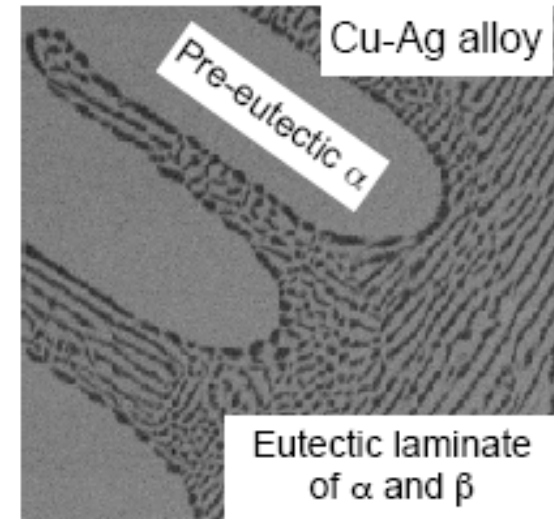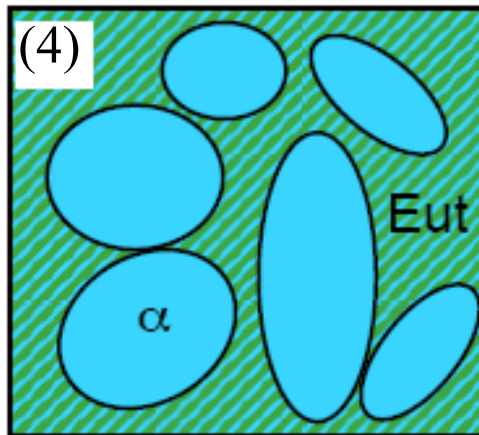
(I) L

(2) L, α

(3) α, L

(4) α, Eut

Cooling curve

Cu-Ag alloy

Pre-eutectic α

Eutectic laminate of α and β

4.2.3. Limiting forms of eutectic phase diagram

1) Complete immiscibility of two metals does not exist.

: The solubility of one metal in another may be so low (e.g. Cu in Ge <10^{-7} at%.)
that it is difficult to detect experimentally, but there will always be a measure of solubility.
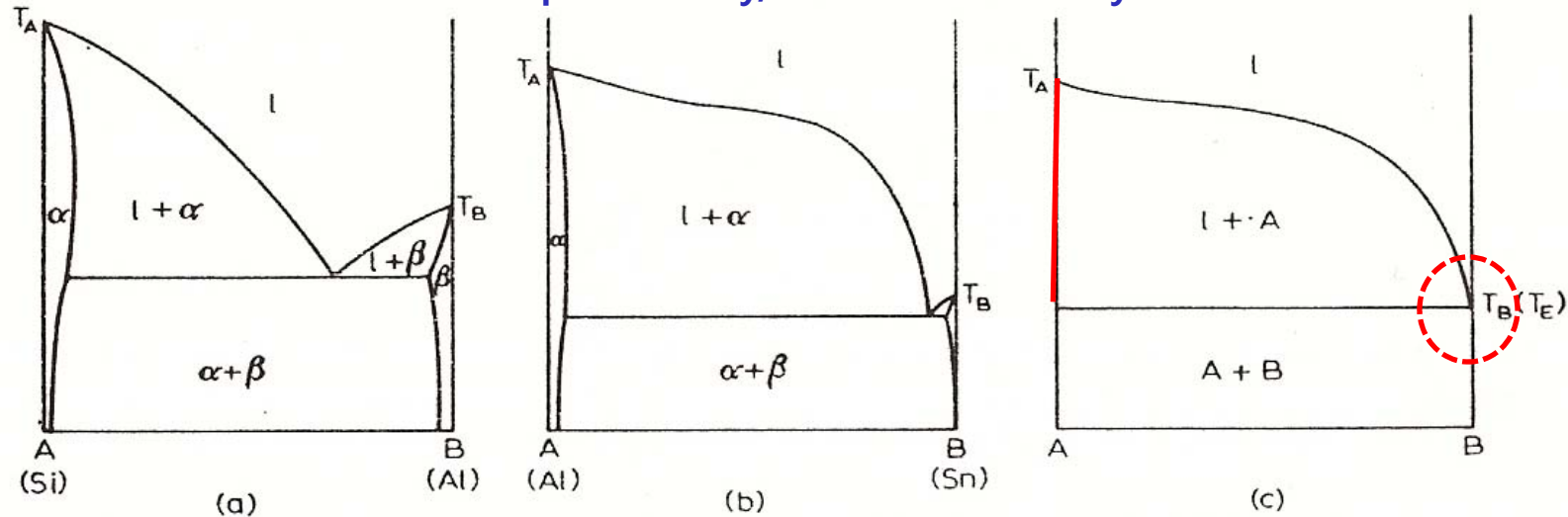

Fig. 53. Evolution of the limiting form of a binary eutectic phase diagram.
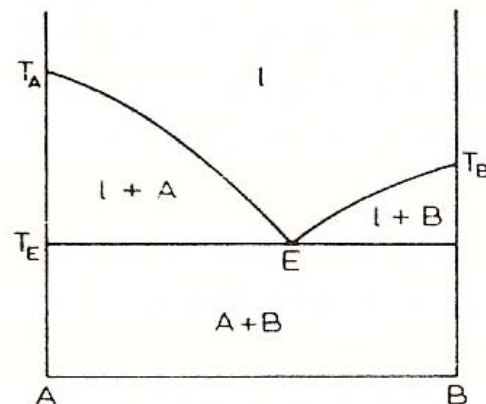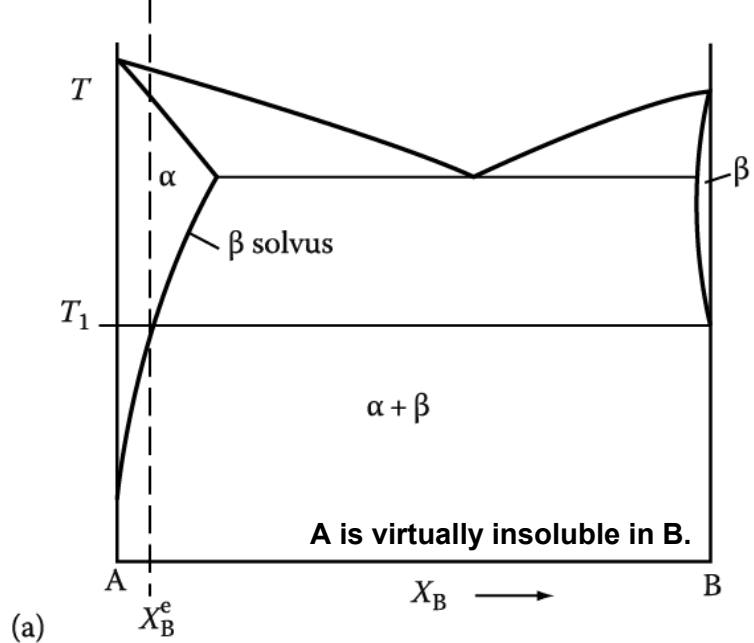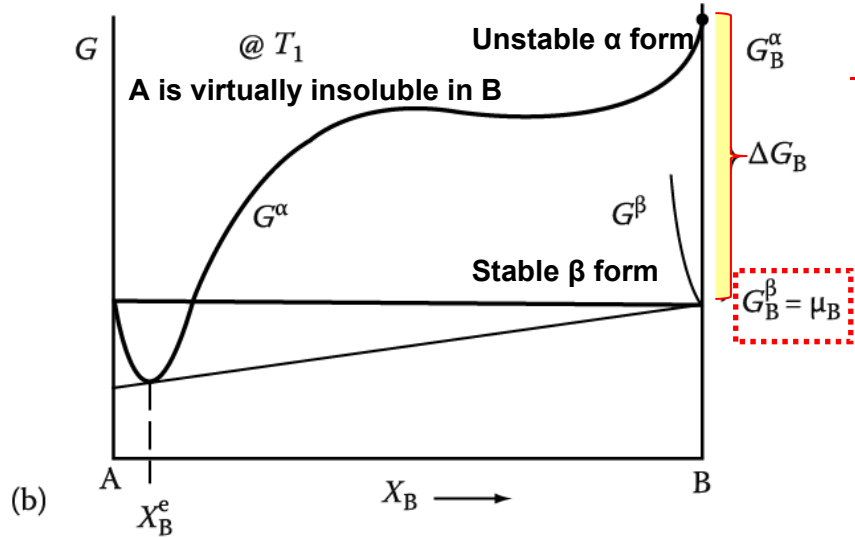

Fig. 54. Impossible form of a binary eutectic phase diagram.

* Effect of T on solid solubility

$$T \uparrow \implies X_B^e \uparrow$$

(b)

@ T_1

Unstable α form

A is virtually insoluble in B

G^α G^β

Stable β form

G_B^α

ΔG_B

$G_B^\beta = \mu_B$

X_B^e

(a)

T

α

β solvus

T_1

$\alpha + \beta$

A is virtually insoluble in B.

X_B^e

$$\mu_B^\alpha = {}^o G_B^\alpha + \Omega(1-X_B)^2 + RT\ln X_B = \mu_B^\beta \simeq {}^o G_B^\beta$$

$$\Delta G_B^{\beta\to\alpha} = {}^0 G_B^\alpha - {}^o G_B^\beta = {}^o G_B^\alpha - \mu_B^\beta = {}^o G_B^\alpha - \mu_B^\alpha$$

$${}^o G_B^\alpha - \mu_B^\alpha = -\Omega(1-X_B)^2 - RT\ln X_B$$

$$\Delta G_B^{\beta\to\alpha} = -\Omega(1-X_B)^2 - RT\ln X_B$$

$$RT\ln X_B = -\Delta G_B^{\beta\to\alpha} - \Omega(1-X_B)^2$$

$$(here, X_B^e \ll 1)$$

$$RT\ln X_B^e = -\Delta G_B^{\beta\to\alpha} - \Omega$$

$$\gg \quad X_B^e = \exp\left(-\frac{\Delta G_B^{\beta\to\alpha} + \Omega}{RT}\right)$$

$$\Delta G_B^{\beta\to\alpha} = \Delta H_B^{\beta\to\alpha} - T\Delta S_B^{\beta\to\alpha} \quad 이므로$$

$$X_B^e = \exp\left(\frac{\Delta S_B^{\beta\to\alpha}}{R}\right)\exp\left(-\frac{\Delta H_B^{\beta\to\alpha} + \Omega}{RT}\right)$$

$$X_B^e = A\exp\left\{-\frac{Q}{RT}\right\}$$

$$T \uparrow \implies X_B^e \uparrow$$

Q : **heat absorbed (enthalpy) when 1 mole of β dissolves in A rich α as a dilute solution.**

* Limiting forms of eutectic phase diagram
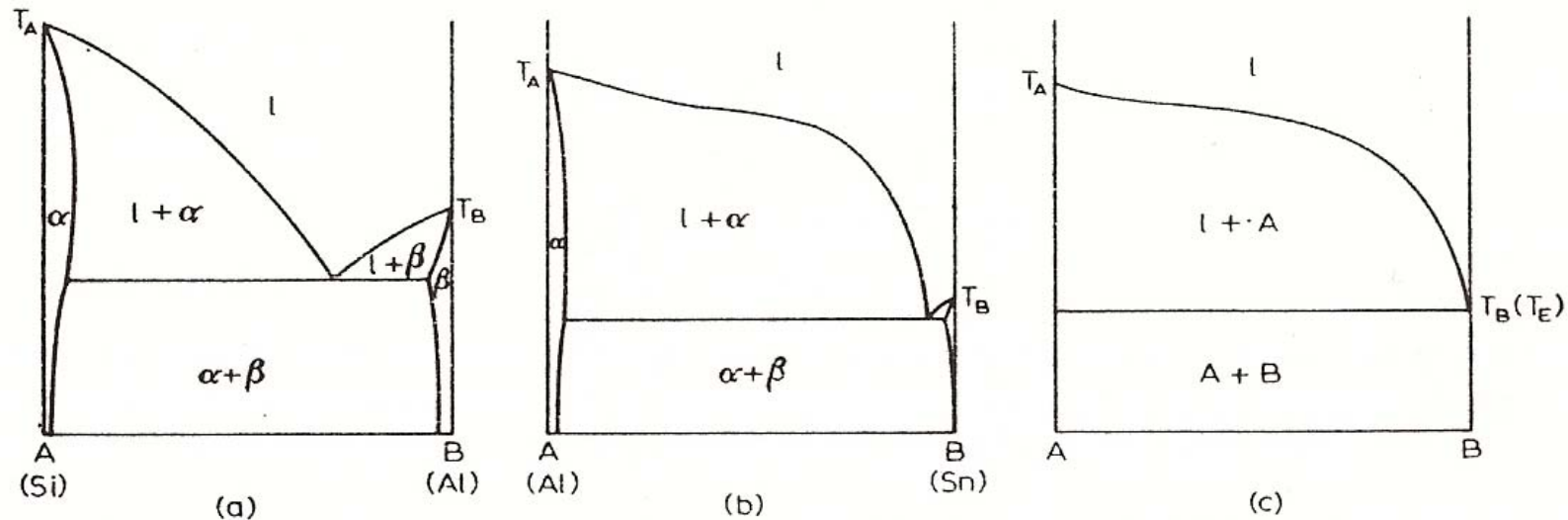
The solubility of one metal in another may be so low.

Fig. 53. Evolution of the limiting form of a binary eutectic phase diagram.

$$X_B^e = A\exp\left\{-\frac{Q}{RT}\right\}$$

a) $\quad T\uparrow \quad \Longrightarrow \quad X_B^e \uparrow$

b) It is interesting to note that, **except at absolute zero,** X_B^e **can never be equal to zero**, that is, no two compo -nents are ever completely insoluble in each other.
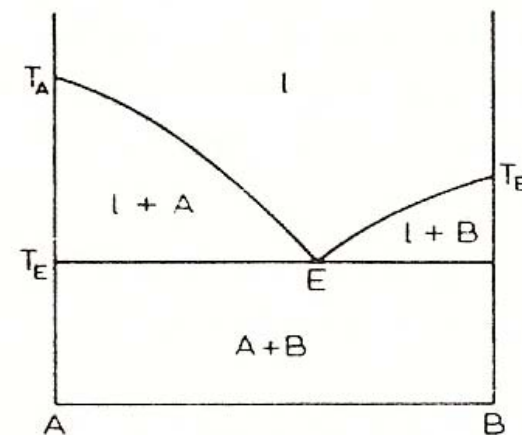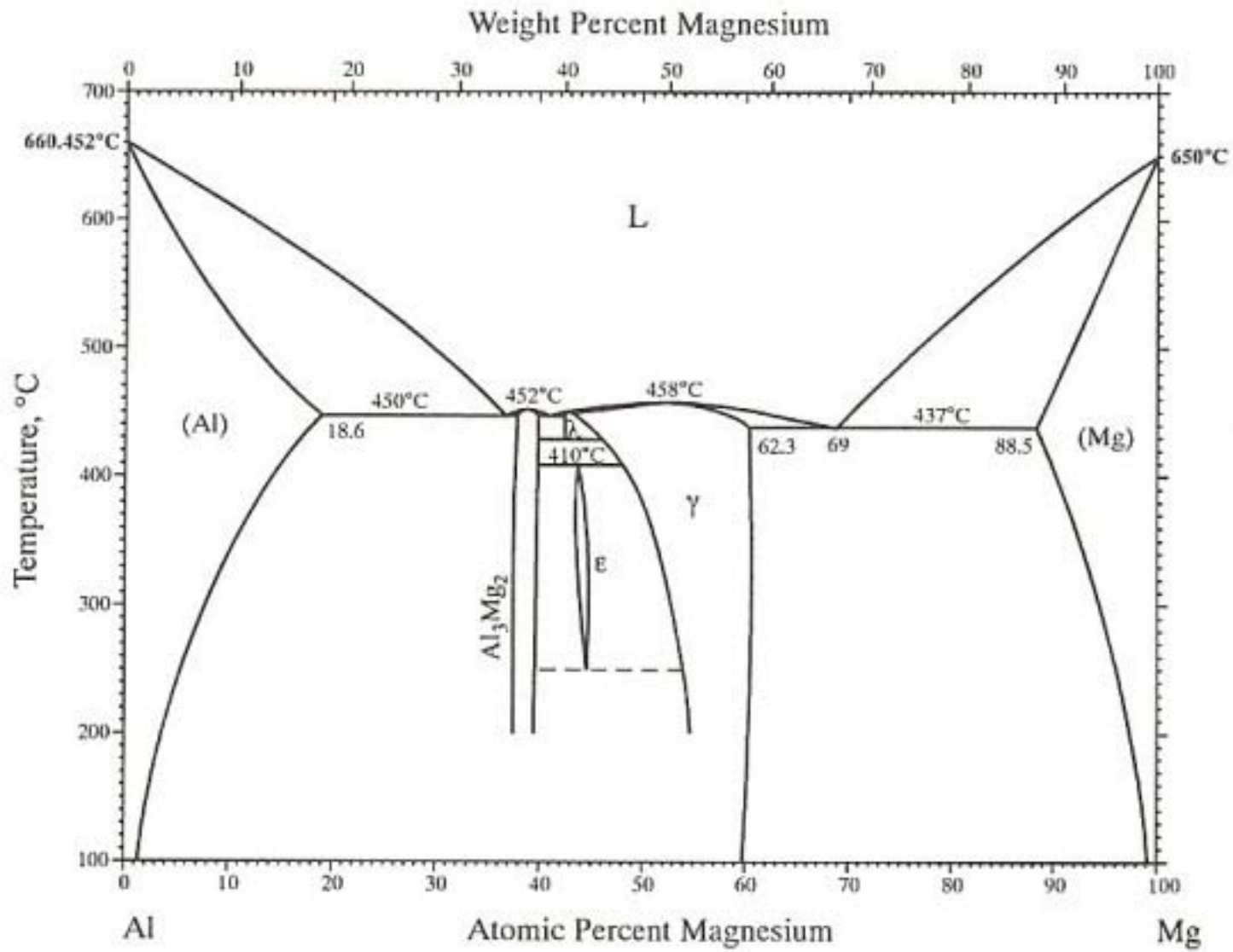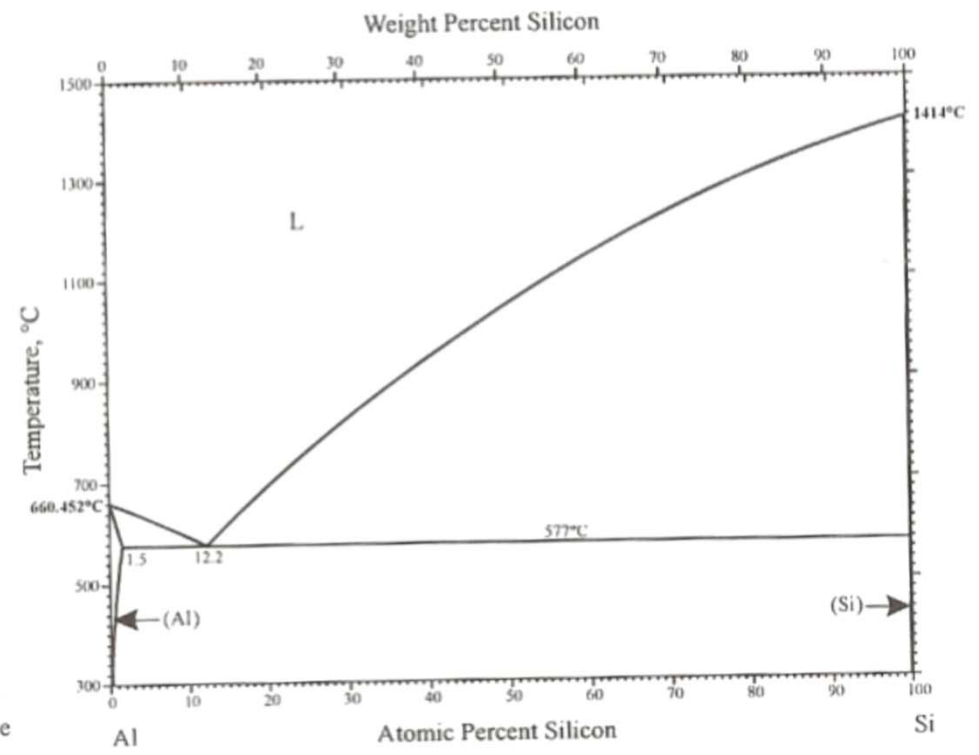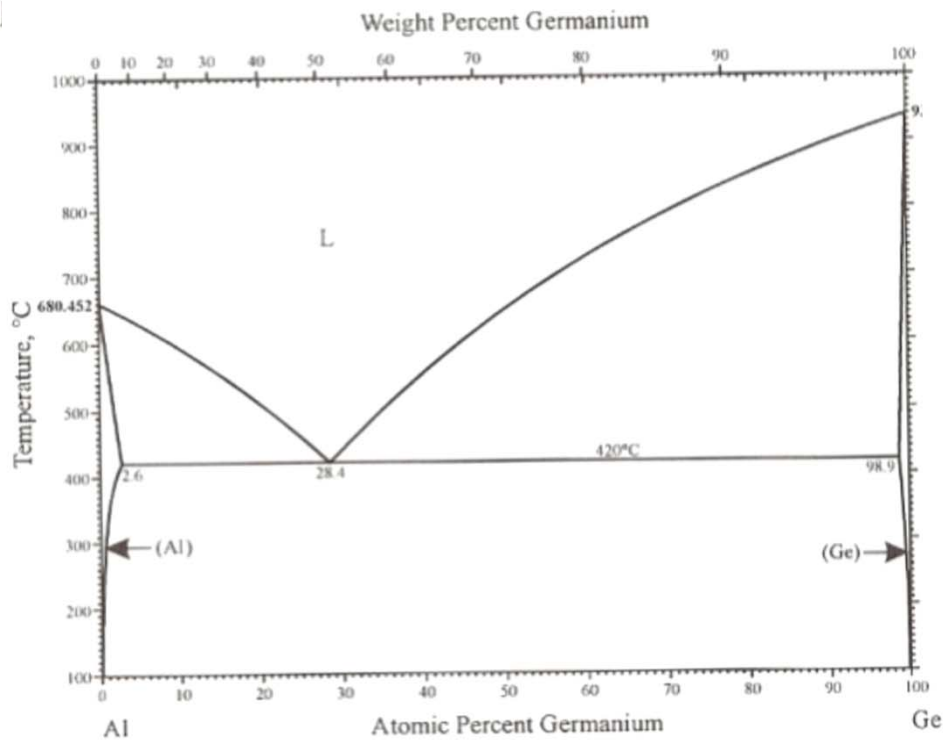

Fig. 54. Impossible form of a binary eutectic phase diagram.

Weight Percent Magnesium

Weight Percent Germanium

Temperature, °C

L

680.452

420°C

2.6   28.4   98.9

(Al)   (Ge)

Al   Atomic Percent Germanium   Ge

Weight Percent Silicon

Temperature, °C

1414°C

L

660.452°C

577°C

1.5   12.2

(Al)   (Si)

Al   Atomic Percent Silicon   Si

37

4.2.5. 2) Retrograde solidus curves

: A maximum solubility of the solute at a temperature between the melting point of the solvent and an invariant reaction isothermal

Solidus curve in the systems with low solubility
Ex) semiconductor research using Ge and Si as solvent metals

A high value of ΔH_B^S (or a large difference in the melting points of the components) is associate with a significant difference in atomic radii for A and B, which can lead to a large strain energy contribution to the heat of solutions.

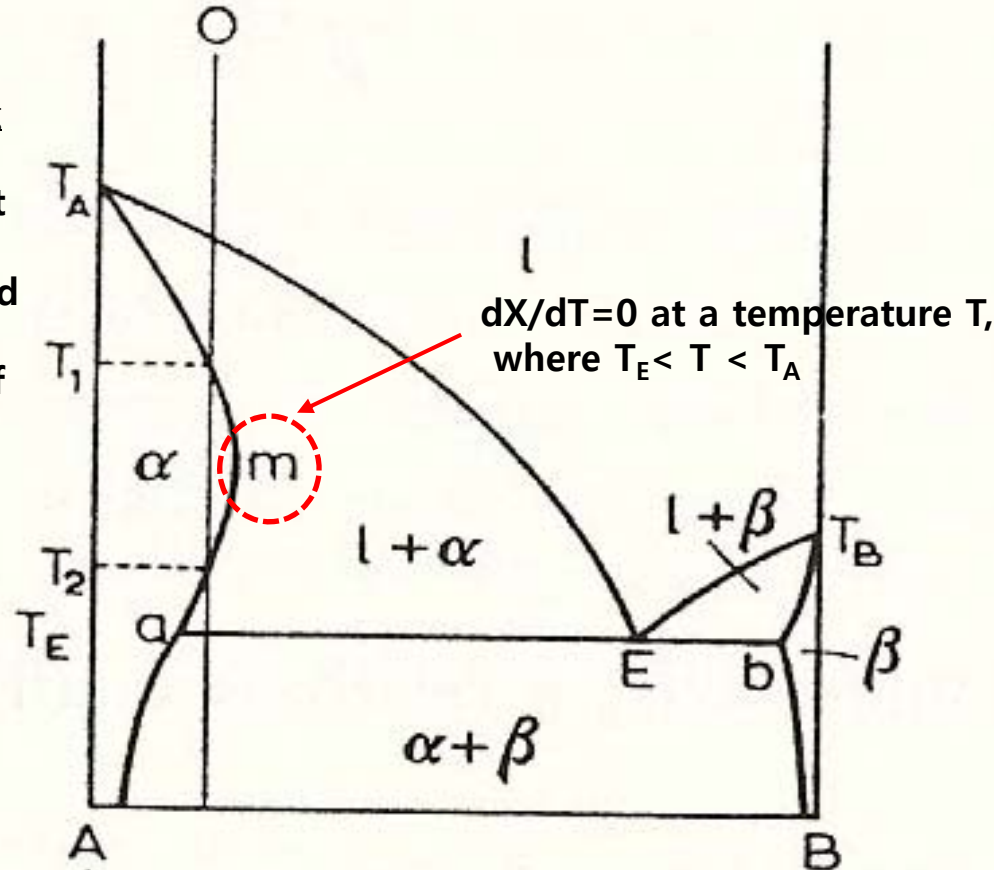dX/dT=0 at a temperature T, where $T_E < T < T_A$

Fig. 57. Partial re-melting associated with retrograde solubility.

Intensive Homework 5: Understanding of retrograde solidus curves from a thermodynamic standpoint

39

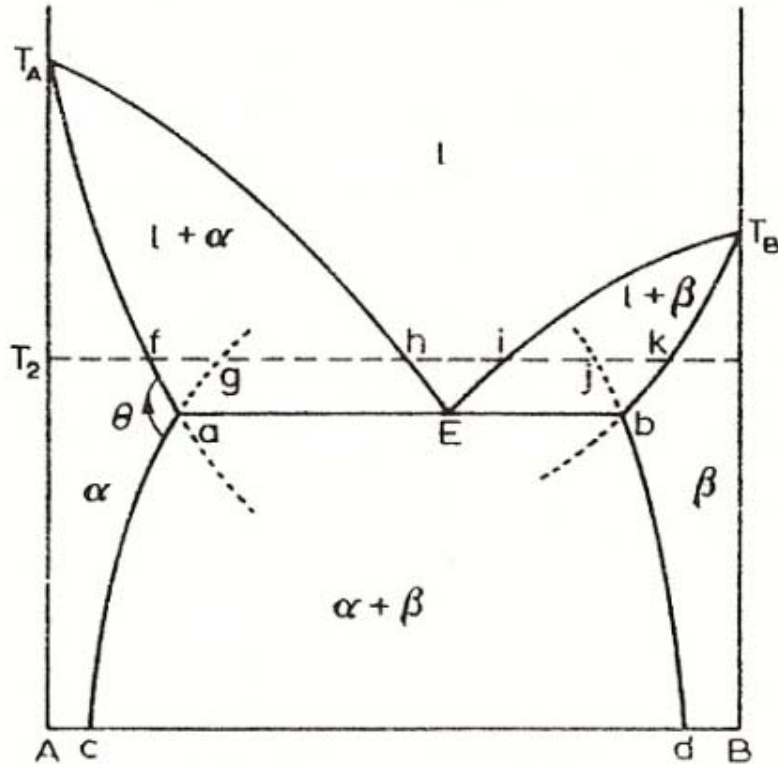## 4.2.5. Disposition of phase boundaries at the eutectic horizontal

Fig. 58. Disposition of phase boundaries at the eutectic horizontal aEb.
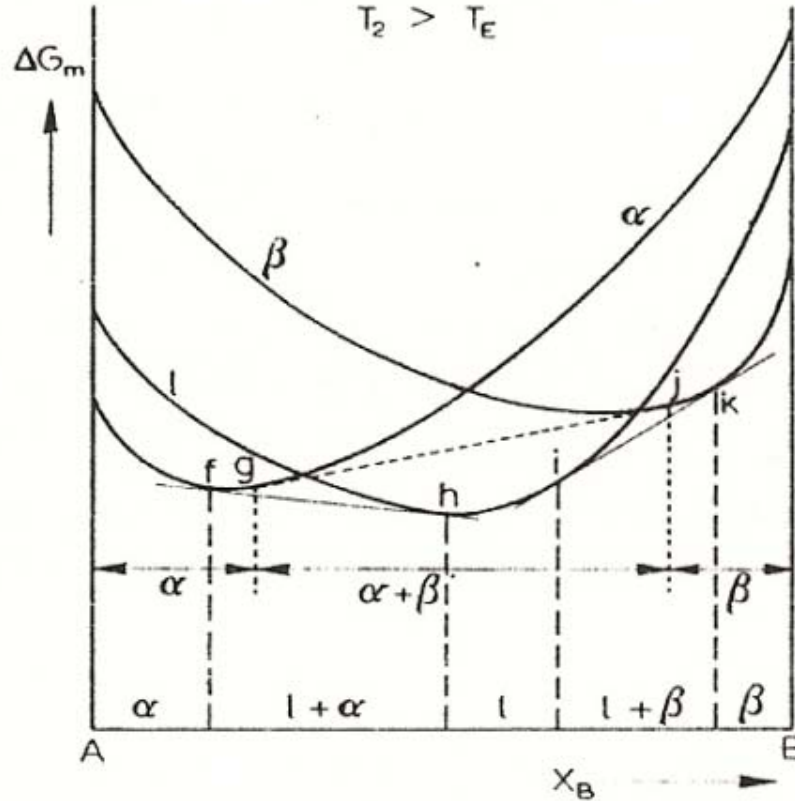

Fig. 59. Free energy curves for the liquid, α and β phases at a temperature T_2 where $T_2 > T_E$.

➡ **3) Ө between solidus and solubility curves must be less than 180°.**

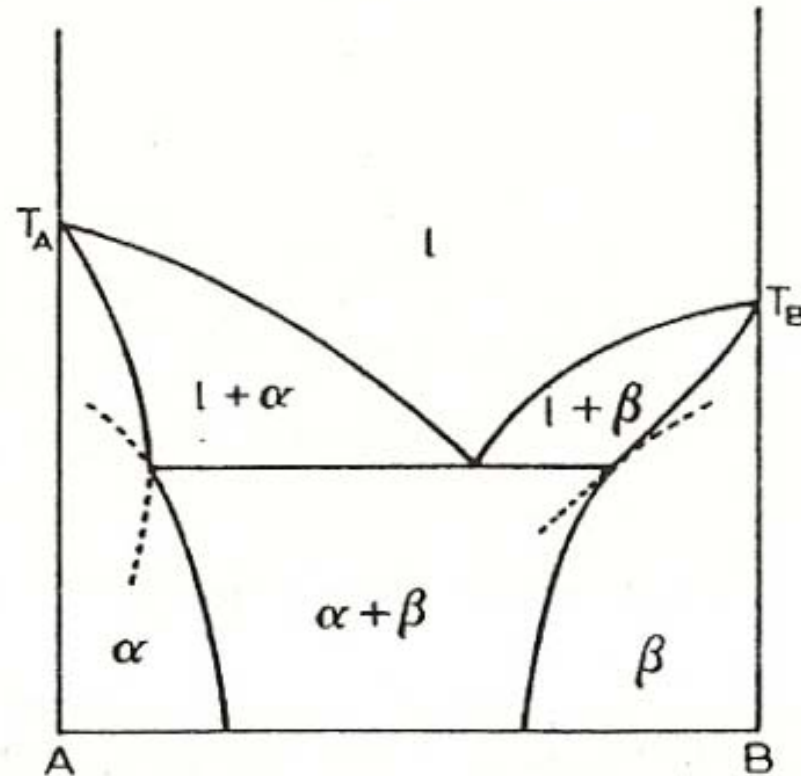## 4.2.5. Disposition of phase boundaries at the eutectic horizontal

Fig. 60. Impossible dispositions of phase boundaries at a eutectic horizontal.

Ө between solidus and solubility curves must be less than 180°.

This is a general rule applicable to all curves which meet at an invariant reaction horizontal in a binary diagram, whether they be eutectic, peritectics, eutectoid, etc., horizontals.

Contents for today's class

- Binary phase diagrams

1) Simple Phase Diagrams

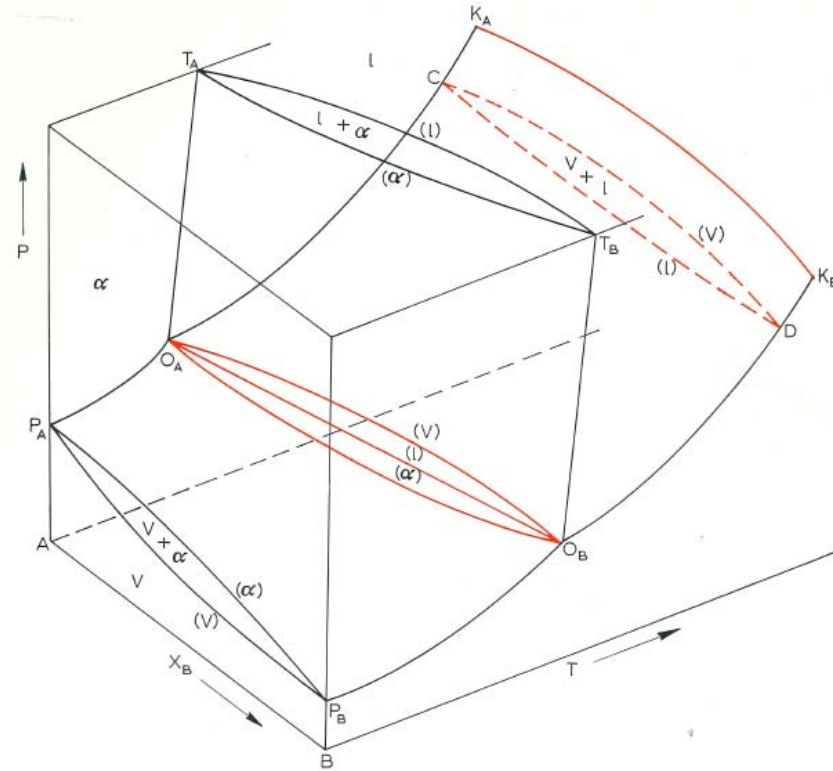* Pressure-Temperature-Composition phase diagram for a system with continuous series of solutions

Fig. 35. Pressure–temperature–composition phase diagram for a system with continuous series of solutions

3) Simple Eutectic Systems

(a) Ideal solution

(b) (c) (d)

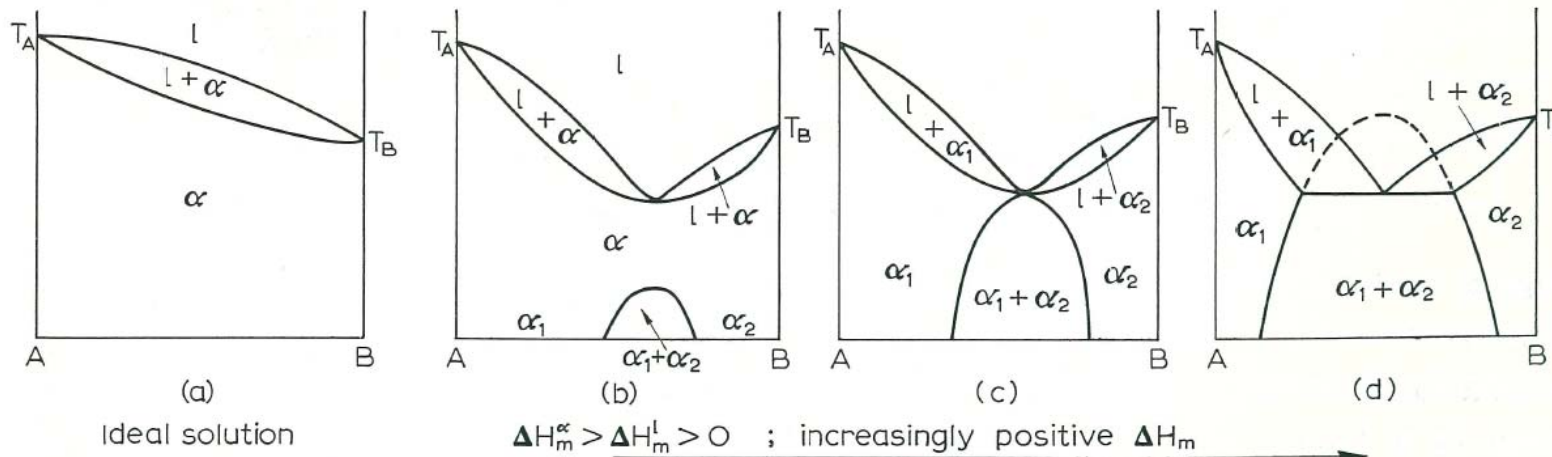$\Delta H_m^{\alpha} > \Delta H_m^{l} > 0$; increasingly positive ΔH_m

Fig. 43. Effect of increasingly positive departure from ideality in changing the phase diagram for a continuous series of solutions to a eutectic-type.

42

By plotting a series of the free energy-composition curves at different temperatures we established the manner in which the phase compositions changes with temperature. In other words, we determined the phase limits or phase boundaries as a function of temperature. A phase diagram is nothing more than a presentation of data on the position of phase boundaries as a function of temperature.
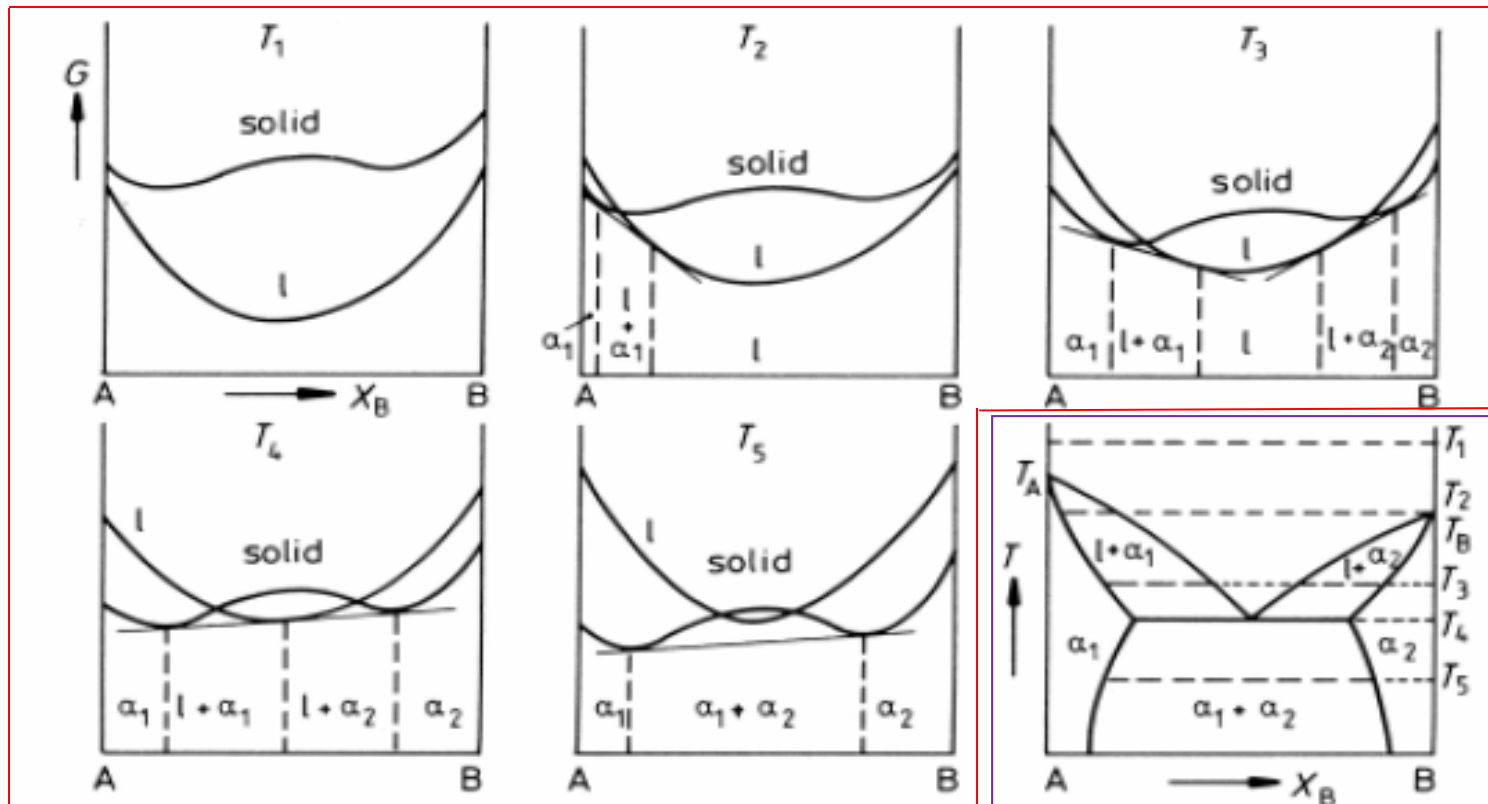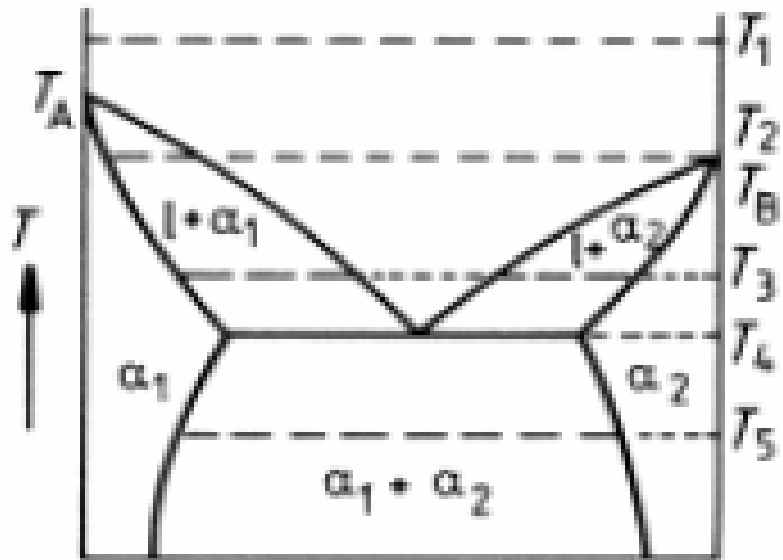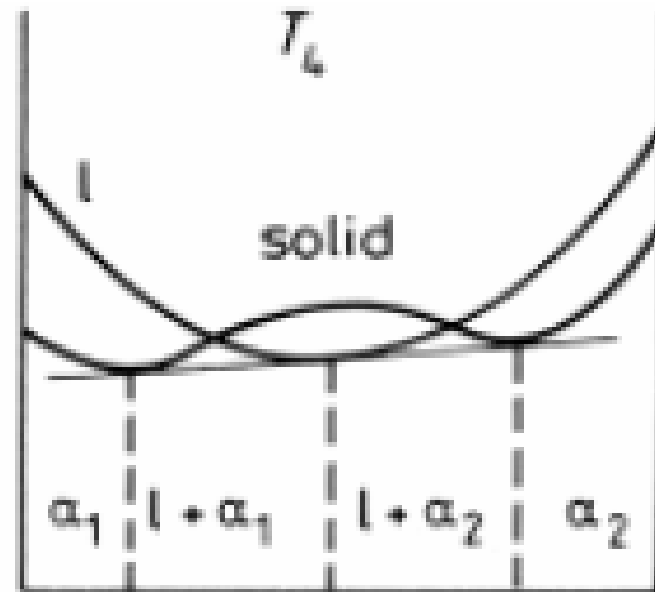

Fig 1.32 The derivation of a eutectic phase diagram where both solid phases have the same crystal structure. (After A.H. Cottrell, *Theoretical Structural Metallurgy*, Edward Arnold, London, 1955,©Sir Alan Cottrell.)
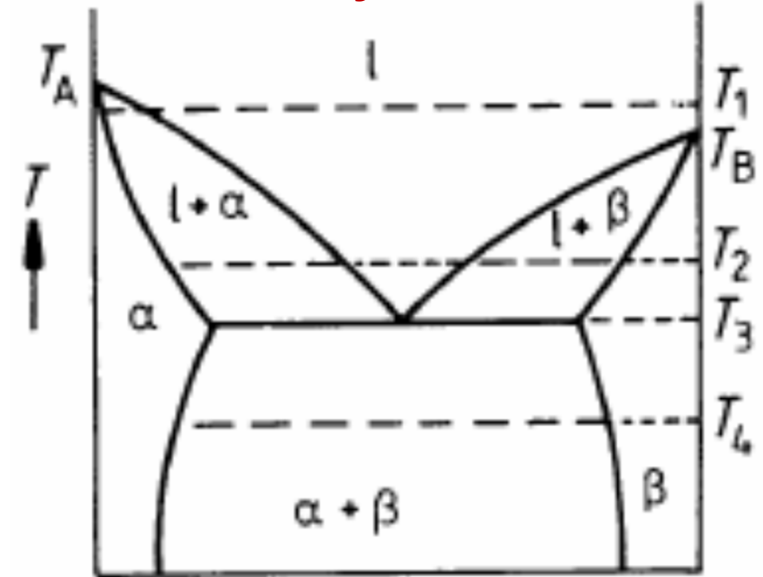
same crystal structure

different crystal structure
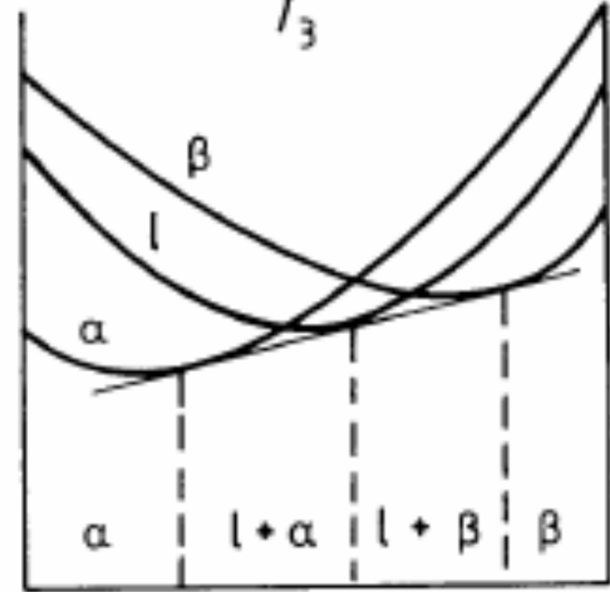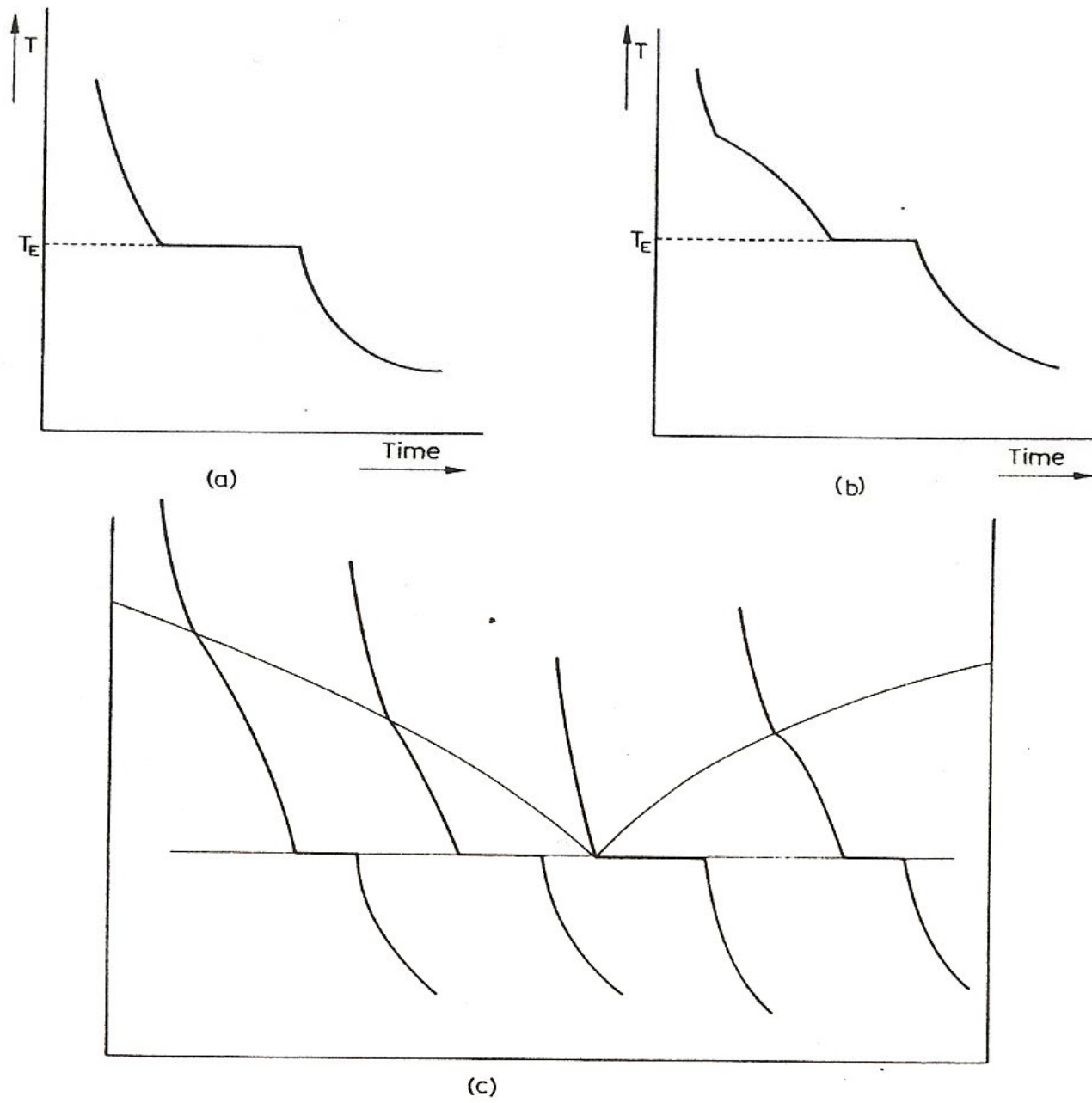
44

Fig. 48. Cooling curve for (a) the eutectic alloy, (b) hypo-eutectic alloy *N*, and (c) a series of alloys, allowing the determination of the liquidus and eutectic horizontal.

45

4.2.3. Limiting forms of eutectic phase diagram

1) Complete immiscibility of two metals does not exist.

: The solubility of one metal in another may be so low (e.g. Cu in Ge <10^{-7} at%.)
that it is difficult to detect experimentally, but there will always be a measure of solubility.
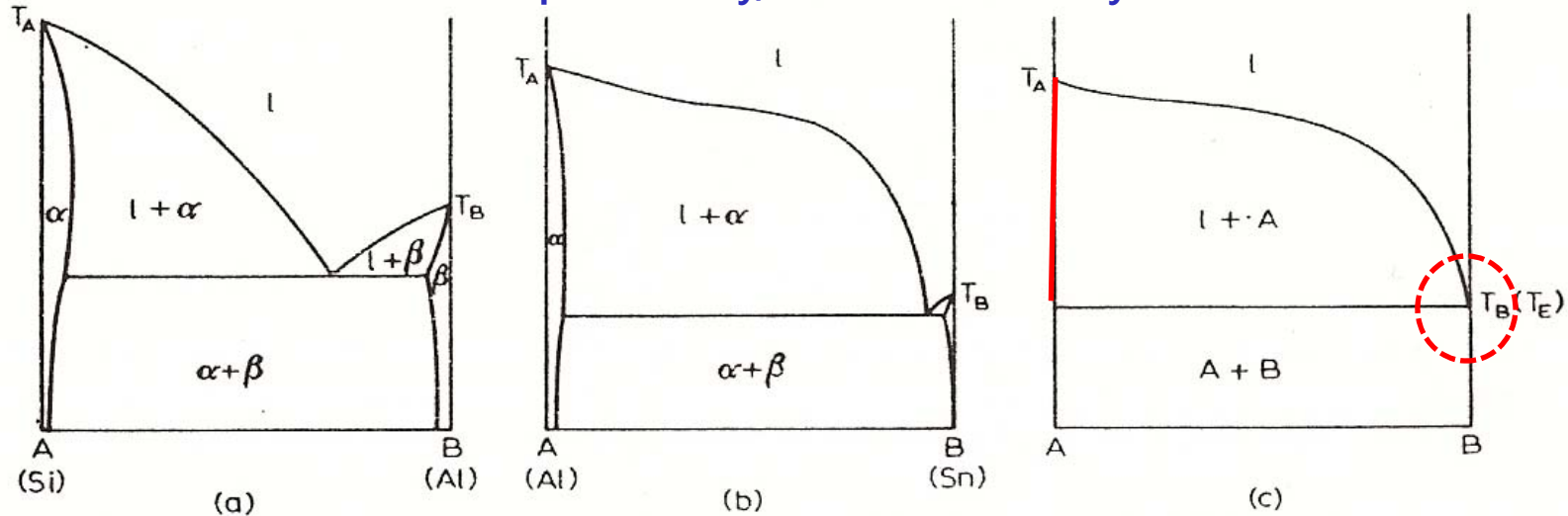

Fig. 53. Evolution of the limiting form of a binary eutectic phase diagram.
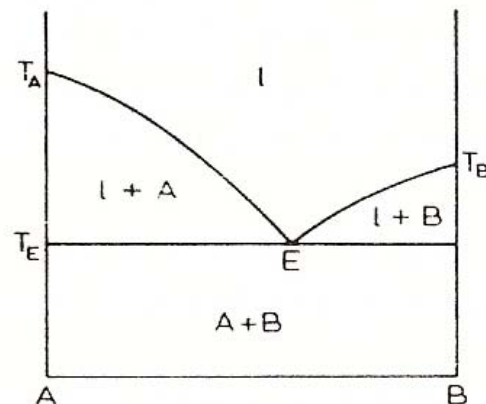

Fig. 54. Impossible form of a binary eutectic phase diagram.

4.2.5. 2) Retrograde solidus curves

: A maximum solubility of the solute at a temperature between the melting point of the solvent and an invariant reaction isothermal

Solidus curve in the systems with low solubility
Ex) semiconductor research using Ge and Si as solvent metals

A high value of ΔH_B^S (or a large difference in the melting points of the components) is associate with a significant difference in atomic radii for A and B, which can lead to a large strain energy contribution to the heat of solutions.
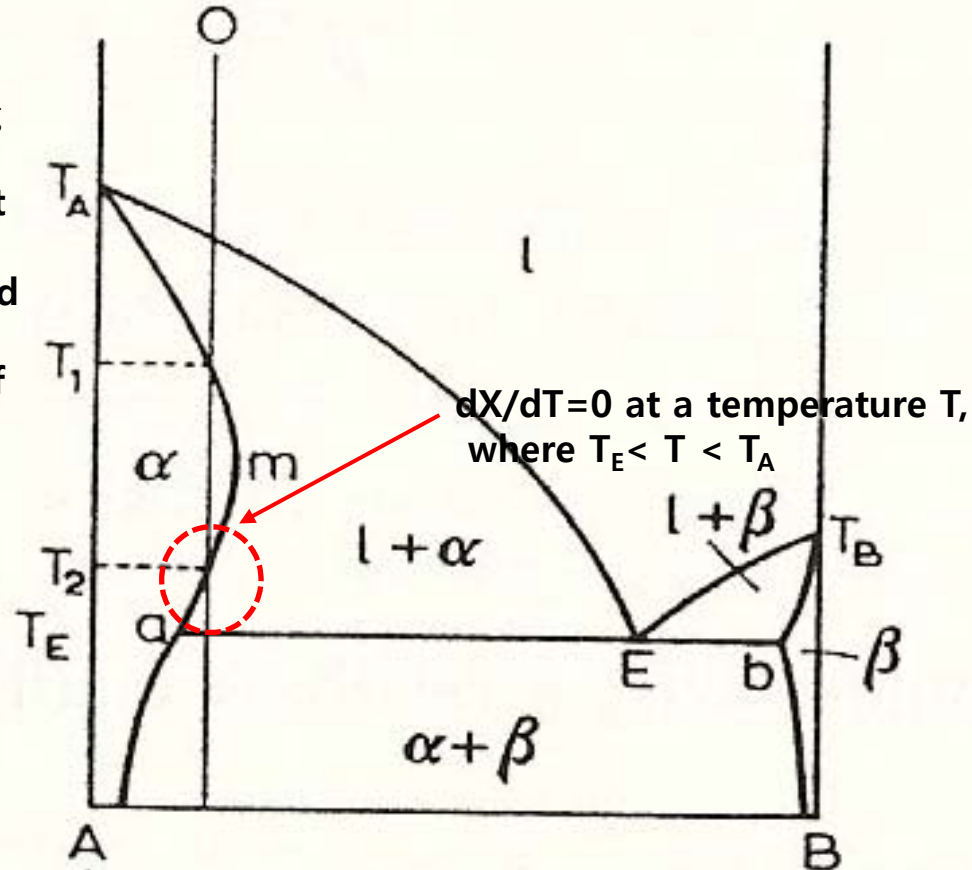
dX/dT=0 at a temperature T, where $T_E < T < T_A$

Fig. 57. Partial re-melting associated with retrograde solubility.

Intensive Homework 5: Understanding of retrograde solidus curves from a thermodynamic standpoint

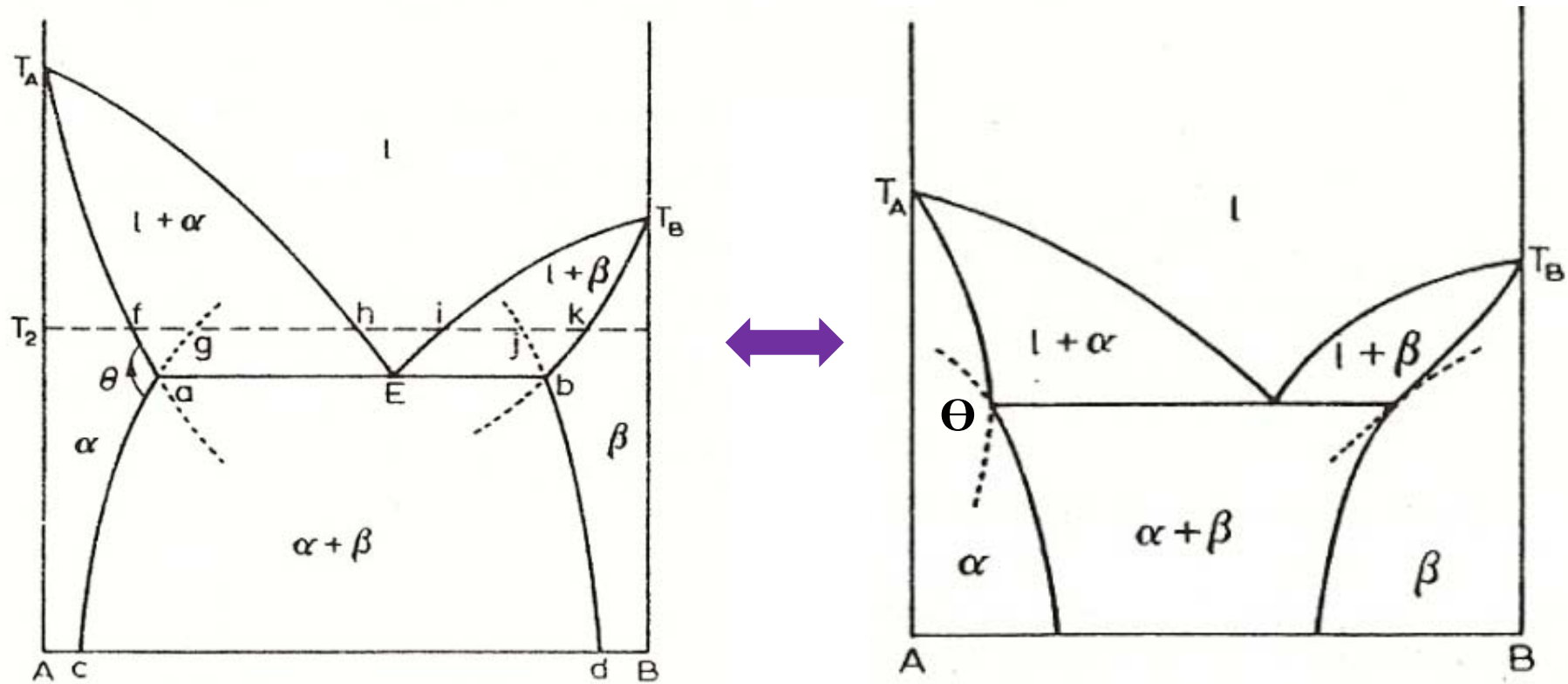## 4.2.5. Disposition of phase boundaries at the eutectic horizontal

Fig. 60. Impossible dispositions of phase boundaries at a eutectic horizontal.

3) Ө between solidus and solubility curves must be less than 180°.

This is a general rule applicable to all curves which meet at an invariant reaction horizontal in a binary diagram, whether they be eutectic, peritectics, eutectoid, etc., horizontals.